South Asian Summer Monsoon Precipitation is Sensitive to Southern Hemisphere Subtropical Radiation Changes

Dipti Swapnil Hingmire[1], Haruki Hirasawa[1], Hansi Alice Singh[1], Philip J. Rasch[2], Soo Kyung Kim[3], Subhashis Hazarika[3], Peetak Mitra[4], and Kalai Ramea[5]

[1]University of Victoria
[2]Pacific Northwest National Laboratory (DOE)
[3]SRI International
[4]Excarta
[5]Planette Inc.

April 16, 2024

Abstract

We study the sensitivity of South Asian Summer Monsoon (SASM) precipitation to Southern Hemisphere (SH) subtropical Absorbed Solar Radiation (ASR) changes using Community Earth System Model 2 simulations. Reducing positive ASR biases over the SH subtropics impacts SASM, and is sensitive to the ocean basin where changes are imposed. Radiation changes over the SH subtropical Indian Ocean (IO) shifts rainfall over the equatorial IO northward causing 1-2 mm/day drying south of equator, changes over the SH subtropical Pacific increases precipitation over northern continental regions by 1-2 mm/day, and changes over the SH subtropical Atlantic have little effect on SASM precipitation. Radiation changes over the subtropical Pacific impacts the SASM through zonal circulation changes, while changes over the IO modify meridional circulation to bring about changes in precipitation over northern IO. Our findings suggest that reducing SH subtropical radiation biases in climate models may also reduce SASM precipitation biases.

South Asian Summer Monsoon Precipitation is Sensitive to Southern Hemisphere Subtropical Radiation Changes

Dipti Hingmire[1], Haruki Hirasawa[1], Hansi Singh[1,5], Philip J. Rasch[2], Sookyung Kim[3,6], Subhashis Hazarika[3,6], Peetak Mitra[3,4], Kalai Ramea[3,5]

[1]School of Earth and Ocean Sciences, University of Victoria, Victoria, BC, Canada
[2]Department of Atmospheric Sciences, University of Washington, Seattle, WA, USA
[3]Palo Alto Research Corporation, Palo Alto, CA, USA
[4]Excarta, Palo Alto, CA, USA
[5]Planette Inc., San Francisco, CA, USA
[6]SRI International, Palo Alto, CA, USA

Key Points:

- We test if biases in southern hemisphere shortwave radiation contributes to biases in South Asian Summer Monsoon Precipitation in the CESM2.
- Reducing incoming shortwave radiation in the subtropical southern hemisphere reduces dry biases over continental South Asia.
- This effect is mostly due to forcing in the South Pacific, with less impact from the Atlantic or Indian ocean.

Corresponding author: Dipti Hingmire, `dhingmire@uvic.ca`

Abstract

We study the sensitivity of South Asian Summer Monsoon (SASM) precipitation to Southern Hemisphere (SH) subtropical Absorbed Solar Radiation (ASR) changes using Community Earth System Model 2 simulations. Reducing positive ASR biases over the SH subtropics impacts SASM, and is sensitive to the ocean basin where changes are imposed. Radiation changes over the SH subtropical Indian Ocean (IO) shifts rainfall over the equatorial IO northward causing 1-2 mm/day drying south of equator, changes over the SH subtropical Pacific increases precipitation over northern continental regions by 1-2 mm/day, and changes over the SH subtropical Atlantic have little effect on SASM precipitation. Radiation changes over the subtropical Pacific impacts the SASM through zonal circulation changes, while changes over the IO modify meridional circulation to bring about changes in precipitation over northern IO. Our findings suggest that reducing SH subtropical radiation biases in climate models may also reduce SASM precipitation biases.

Plain Language Summary

Precipitation from South Asian Summer Monsoon (SASM) is of high significance to the livelihoods of over a billion people. As the global climate continues to evolve, it is essential to have a clear understanding of the possible future changes to the SASM. However, current state-of-the-art climate models have difficulties in simulating climatological mean SASM precipitations. Here we study sensitivity of SASM precipitation to subtropical southern ocean radiation as one of the possible causes of SASM precipitation bias. Our experiments indicate that SASM precipitation is sensitive to southern hemisphere subtropical radiation changes particularly to those in subtropical Pacific. These findings imply that improving southern hemisphere subtropical radiation biases might improve SASM precipitation simulations in climate models.

1 Introduction

The South Asian Summer Monsoon (SASM) is a highly influential monsoon system, known for its strength, spatial extent, and significance to the livelihoods of over a billion people. Future greenhouse gas forcing is projected to increase SASM precipitation, but the magnitude and pattern of these changes remain uncertain (Katzenberger et al., 2021; Kumar et al., 2023). Earth System Models (ESMs) serve as the primary means of projecting these changes, but ESMs have long-standing biases in simulating the SASM's climatological precipitation intensity, spatial pattern, and seasonality, among other elements (Mitra, 2021; Konda & Vissa, 2022; Rajendran et al., 2022). These biases have been attributed to various sources, including errors in representation of orography (Boos & Hurley, 2013), land-atmosphere interactions (Ashfaq et al., 2017), air-sea interactions (Annamalai et al., 2017; Hanf & Annamalai, 2020), and sea surface temperatures over the Indian Ocean (Levine et al., 2013; He et al., 2022). ESMs participating in the Coupled Model Intercomparison Project 6 (CMIP6) better simulate the SASM compared to previous generations of models, but significant biases persist (Gusain et al., 2020; Choudhury et al., 2021).

The Community Earth System Model 2 (CESM2) (Danabasoglu et al., 2020), like other climate models, has systematic biases in simulating SASM precipitation. Figure 1a displays the June to September (JJAS) precipitation and lower tropospheric circulation biases for the 1979-2014 period compared to observations and reanalysis. CESM2 does not produce enough precipitation in two regions of the SASM system: (1) over the central land region between 20°-30°N, and (2) over the Indian Ocean between 10°S-0°N with dry biases of 2-4 mm/day over both regions. Between these two dry biased areas, there is a region of excessive precipitation (4-6 mm/day) in the northern Indian ocean surrounding the South Asian landmass producing a meridional dry-wet-dry bias pattern.

The model also tends to overestimate precipitation over the high orography of the Eastern Himalayas, Southeast Asia, and the Maritime continent.

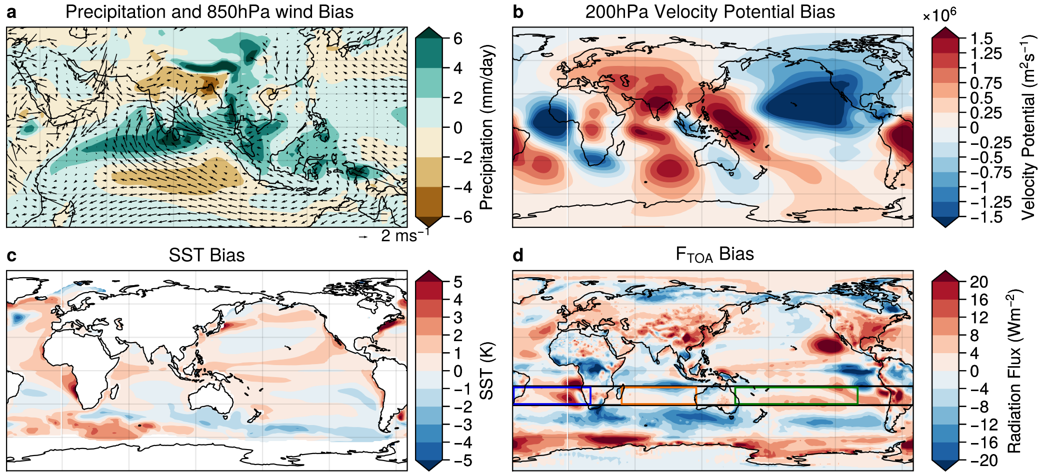

Figure 1. Existing biases in CESM2: Ensemble mean bias of 11 members of CESM2 historical simulations from CMIP dataset in (a) JJAS precipitation, and 850 hPa wind with respect to GPCP (Adler et al., 2018) and ERA5 (Hersbach et al., 2020), respectively; (b) JJAS 200 hPa velocity potential relative to ERA5; and (c) annual mean SST relative to ERSST (Huang et al., 2015); and (d) annual mean net downward top-of-atmosphere (F_{TOA}) radiation flux relative to CERES-EBAF (Loeb et al., 2018). Biases are calculated based on climatology of period 2004-2014 for F_{TOA} and 1979-2014 for all other variables. Boxes in panel d show the specific region where CDNC perturbations are applied for Atlantic (ATL, blue), Indian Ocean (IND, orange), Pacific (PAC, green) and Zonal (ZON, black) experiments.

SASM biases are linked to biases in the regional circulation, which partly arise from local Sea Surface Temperature (SST) biases (Annamalai et al., 2017; He et al., 2022). In CESM2, lower tropospheric winds are biased southeasterly and southerly over the equatorial Indian ocean and parts of Arabian Sea (Figure 1a) and are biased northwesterly over Indian land regions and the Bay of Bengal. Figure 1b displays the upper troposphere circulation bias in terms of the 200hPa velocity potential (VP200). The VP200 bias is greatest over the land regions of India and south of the equator up to 10°S. These positive VP200 biases correspond to subsidence and weaker convergence at lower tropospheric levels, thereby creating dry biases. CESM2 also displays positive SST biases in the tropics globally, which affects the Walker circulation and thus the SASM (Walker, 1923; Jain et al., 2021).

An emerging view is that regional tropical monsoons are local manifestations of seasonal Intertropical Convergence Zone (ITCZ) shifts, and are an important feature of an energy-constrained global circulation (Bordoni & Schneider, 2008; Biasutti et al., 2018; Hill, 2019; Geen et al., 2020). SASM variability in particular is strongly linked to seasonal migrations of the ITCZ over the Indian subcontinent (Gadgil, 2018; Hari et al., 2020). These seasonal ITCZ migrations are in turn driven by inter-hemispheric energy gradients, as the Hadley circulation, and thus the ITCZ shift, towards the warmer hemisphere to transport excess energy to the opposite hemisphere (Kang et al., 2009; Schneider et al., 2014). Thus, a systematic Absorbed Solar Radiation (ASR) bias could alter this inter-hemispheric energy gradient, thereby disrupting this seasonal ITCZ migration and inducing biases in the monsoon. While ASR biases over the Southern Ocean have been reduced in the latest generation of climate models (Kay et al., 2012; Bodas-Salcedo et al., 2014; Zhao et al., 2022), positive radiation biases still exist over the subtropical Southern Hemisphere (SH) oceans in many ESMs (Li et al., 2013, 2020). In CESM2, the midlatitude SH displays a negative net downward top-of-atmosphere (F_{TOA}) radiation bias while the subtropical SH has a positive F_{TOA} bias between 15°-30°S (Figure 1d), which may be due to insufficient low cloud cover (Xiao et al., 2014) and too weak stratocumulus cloud feedbacks (Kim et al., 2022). This positive SH subtropical F_{TOA} bias is greatest over the Atlantic and Pacific Oceans, but is relatively small in the Indian Ocean.

In the present study, we aim to address the following: does improving SH subtropical radiation biases impact ITCZ position and the simulation of the SASM? And if so, by what mechanism? To test this, we perform CESM2 experiments where we decrease ASR in SH regions with high ASR biases by changing the cloud albedo. We change the cloud properties by prescribing the Cloud Droplet Number Concentration (CDNC) that influences the cloud microphysics and radiation. Our results indicate that reducing ASR biases over the subtropical SH modestly improve SASM precipitation biases over the Indian subcontinent.

2 Methods

To understand the effect of reducing SH ASR biases on SASM, we performed a series of experiments with the Community Earth System model 2 (CESM2, Danabasoglu et al., 2020), the latest generation ESM developed by the National Center for Atmospheric Research and collaborators. Our configuration uses CAM6 for atmosphere, POP2 for ocean, CLM5 for land and CICE5 for sea ice. In our experiments, we perturbed the radiative fluxes in CESM2 by prescribing the in-cloud liquid CDNC at all vertical levels where liquid and mixed phase clouds exist over oceanic regions in the SH subtropics. This reduces the average cloud droplet radius, increasing cloud albedo and lifetime, and thus reducing ASR.

First we conducted Fixed Sea Surface Temperature (Fixed-SST) experiments to identify the sensitivity of F_{TOA} fluxes to CDNC, and determined the CDNC values that would minimize the ASR bias compared to observations. We then carried out five fully coupled simulations with repeating year-2000 forcings - one control simulation (2000CNT) without any perturbations and four experiments which introduced the identified CDNC perturbations in different regions of SH subtropics (15°-30°S) (listed in Table 1). The first three simulations introduced a perturbation in each of the Atlantic (ATL) [50°W-20°E], Indian (IND) [48°-115°E], and Pacific (PAC) [150°E-80°W] oceans and the fourth simulation perturbed ocean regions in the entire zonal band (ZON) (180°W-180°E). We set the CDNC value to 150 cm^{-3} for ATL and 75 cm^{-3} for the PAC, IND, and ZON experiments. When compared to existing CESM2 F_{TOA} bias with EBAF (Figure 1d), the applied perturbations correct most of the F_{TOA} bias in the subtropical SH Atlantic but over the subtropical SH Pacific and Indian Ocean the perturbation exceeds F_{TOA} bias, resulting in a negative bias (Figure S1 and Table 1). Fixed-SST experiments were run for 7 years and fully coupled experiments for 150 years. We calculate the response as the climatological average difference between perturbation experiment and control run for the last 5 and 30 years of the fixed-SST and fully coupled simulations respectively. Statistical significance of response is tested using the Student's t-test with $p < 0.05$.

2.1 ITCZ position

We compute the ITCZ latitude as the centroid of the zonal-mean, time-mean precipitation between 30°N and 30°S (Frierson & Hwang, 2012; Voigt et al., 2016). As demonstrated by Atwood et al. (2020), regional rainbelts do not shift uniformly in response to hemispherically asymmetric forcing, therefore we also analyse regional ITCZs in the Atlantic (10°W–40°W), Indian (70°E -90°E) and Pacific (110°E–100°W) oceans.

Table 1. Details of coupled CESM2 experiments used in this study

Experiment name	Abbreviation	CDNC perturbation applied	Perturbation Region	Global F_{TOA} response in W/m2	Regional F_{TOA} response in W/m2 (Existing CESM2 bias)
Control	2000CNT	0	0	0	0
Atlantic	ATL	150 cm^{-3}	50°W-20°E, 15°-30°S	-0.21±0.87	-5.43 ±1.28 (5.77 ±0.19)
Indian Ocean	IND	75 cm^{-3}	48°-115°E, 15°-30°S	-0.08±0.88	-5.71 ±1.5 (-2.50 ±0.2)
Pacific	PAC	75 cm^{-3}	150°E-80°W, 15°-30°S	-0.39 ±0.85	-7.27 ±1.21 (3.31 ±0.3)
Zonal	ZON	75 cm^{-3}	180°W-180°E, 15°-30°S	-0.53±0.88	-4.34 ±1.23 (2.43 ±0.23)

3 Results

3.1 Energetically constrained global precipitation response

All experiments show energy being transported towards the SH subtropics, where we created an ASR depression by artificially increasing CDNC, producing increasing northward transport between 60-30 S (positive values) and southward transport between 15S-30N (negative values) (Figure 2a). The experiments show similar responses in terms of direction of transport however the magnitude of response differs. The magnitude is proportional to the F_{TOA} anomaly e.g. ZON shows highest absolute F_{TOA} and total energy transport response while as IND shows least absolute values for the both (See Table 1 and Figure 2a). Most of this energy transport is carried out by atmospheric transport as shown by Atmospheric Energy Transport (AET) response in Figure 2b. Experiments show varied ocean heat transport responses but the changes are one order less than that of AET (Figure 2c). These results confirm the findings of Xiang et al. (2018) that atmosphere transports energy more effectively than oceans when energy perturbations are applied at lower latitudes.

Following the energetics framework (Kang et al., 2009; Schneider et al., 2014; Donohoe et al., 2013), AET changes bring about changes in precipitations as shown in Figure 2d. All the experiments show increase of precipitation in the tropical northern hemisphere and reductions in the tropical SH, indicating northward migration of the ITCZ. Consistent with AET response, the precipitation change is larger in ZON and PAC and weaker in IND and ATL. In Figure 2e and 2f, we quantify these ITCZ shifts and their biases. In CESM2, the annual mean ITCZ position has northward bias of 0.25 ° (Figure 2e). However, this bias is regionally and seasonally dependent. In the context of the SASM we are interested in JJAS ITCZ location in Indian Ocean, which is biased 1.2° southwards (Figure 2f). All of the experiments show significant northward shifts in respective regional annual and JJAS global ITCZs (Figure 2e and 2f). Notably, IND, PAC and ZON show significant northward shifts in annual and JJAS mean ITCZ over the Indian Ocean. Thus, as hypothesized, our experiments show that the ITCZ responses followed the energetic framework.

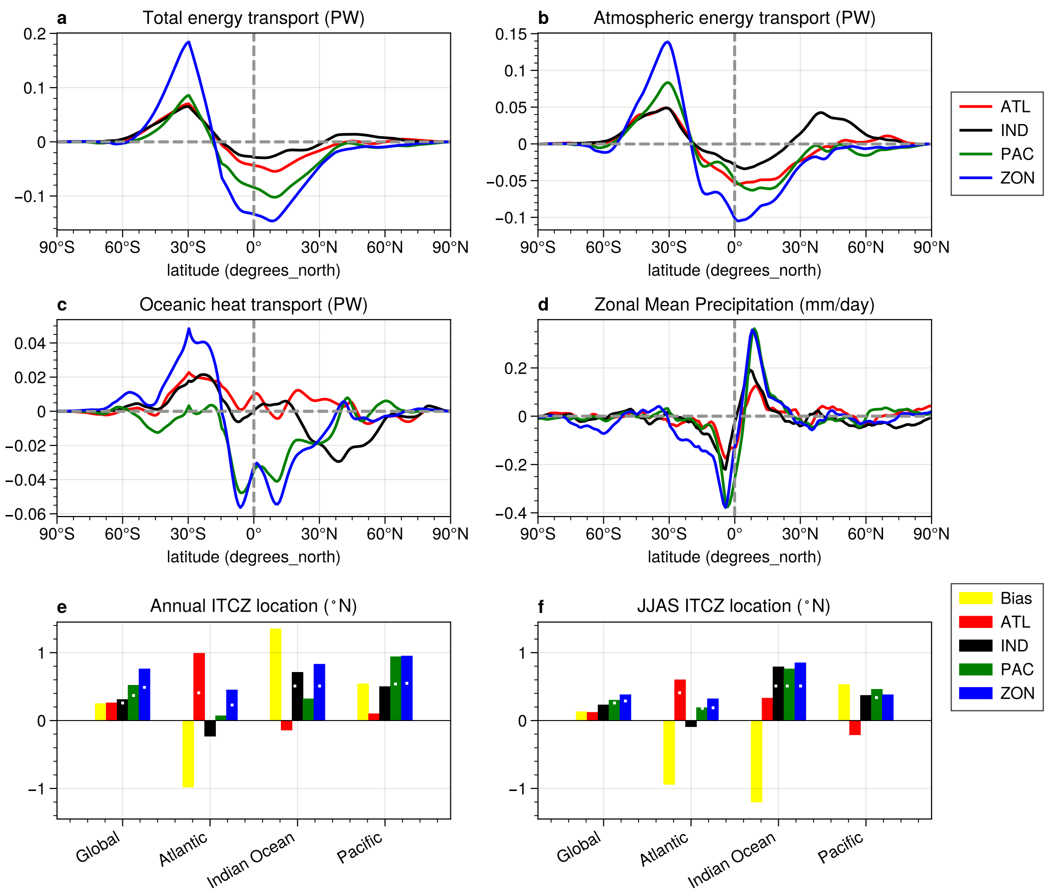

Figure 2. **Global energetic and precipitation response:** Zonal mean response of (a) total energy tranport, (b) atmospheric energy transport, (c) ocean heat transport, (d) annual mean precipitation, (e) annual and (f) JJAS ITCZ position shift in fully coupled simulation for ATL (red), IND (black), PAC (green) and ZON (blue) experiments and CESM2 existing biases (yellow in e and f panels). White dots in panels e and f indicate the statistically significant shifts of ITCZ.

3.2 SASM precipitation response

We now consider how the ITCZ shifts influence SASM precipitation. Despite the similar effect of IND, PAC and ZON on the JJAS Indian Ocean ITCZ, the SASM precipitation response differ considerably in these experiments (Figure 3). Reducing ASR in the PAC causes significant precipitation increases over the central continental India. This stands out from the other experiments and contributes to a reduction of the JJAS dry bias over this region (Figure 3c; see Figure 1a for bias). However, the increase in precipitation of 1-2 mm/day for the PAC is only a partial compensation for the 2-4 mm/day dry bias of SASM precipitation in CESM2 over this region. For the ATL experiment, whose main ITCZ response is in the Atlantic, the JJAS SASM precipitation change is largely non-significant over the SASM region (Figure 3a). It is also interesting to see that IND experiment moves the annual and JJAS ITCZ northwards (Figure 2e and 2f) and produces precipitation decrease of 1-2 mm/day (Figure 3b) south of equator thus adding to JJAS SASM dry bias over there (Figure 1a). The ZON experiment is similar to IND experiment: significant precipitation increase of 1-2mm/day add to existing wet bias over oceanic regions surrounding Indian land and precipitation decrease of 1mm/day add to

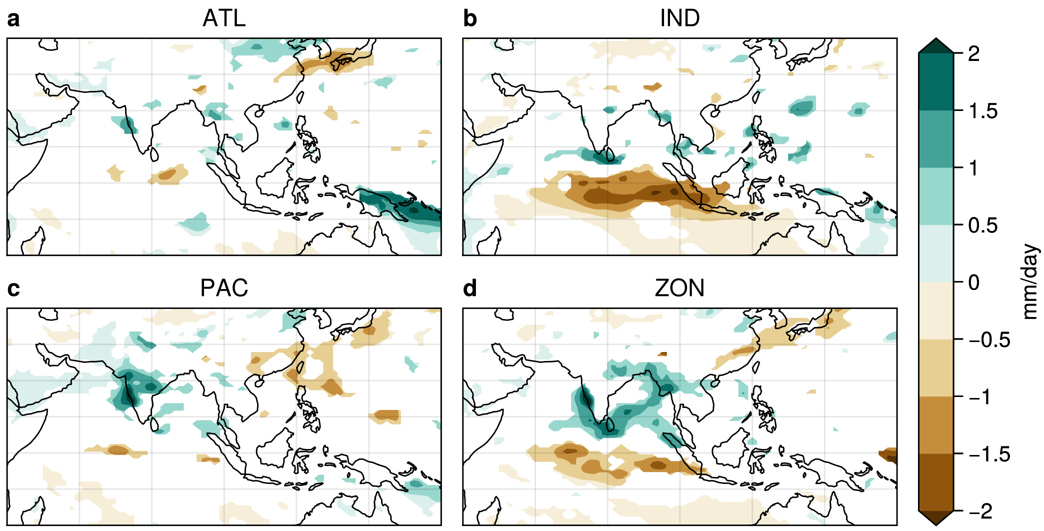

Figure 3. SASM precipitation response: JJAS precipitation response (at simulation period 121-150 years) in fully coupled simulation for experiments (a) ATL, (b) IND, (c) PAC and (d) ZON. Non-significant responses (at level of significance 0.05) are masked in white.

dry biases (Figure 3d) south of the equator. It also reduces dry bias of a small portion over central India east of 80°E. To better decipher these intriguing SASM precipitation responses in different experiments we further explore the large-scale circulation changes in each of these experiments.

3.3 Large-scale circulation response

Panels a-d in Figure 4 show lower tropospheric circulation and associated moisture divergence for each of the experiments. For IND and ZON, the 850hPa wind responses add to existing southeasterly and southerly biases in the equatorial Indian Ocean and parts of the Arabian sea (Figure 4b and d, see Figure 1a for bias). The important wind response of PAC is a southeasterly response over land regions of central India (Figure 4c) which reduces northwesterly circulation bias (Figure 1a). In tandem with lower tropospheric circulation changes, we observe that moisture convergence increases over Indian land region for PAC but over the surrounding oceanic regions for ZON and IND (Figure 4b,c and d). The ATL shows statistically significant increase in lower tropospheric westerlies and the moisture convergence along the west coast (Figure 4a) over a small region. The improved representation of lower level winds and increased moisture flux convergence over central continental India in PAC, contributes to a partial reduction of the dry precipitation bias over this region.

The SASM regional circulation is tightly linked to the large-scale Hadley circulation in the meridional plane and the Walker circulation in the zonal plane (Goswami & Chakravorty, 2017). ZON and IND, show strengthening of the meridional overturning circulation with enhanced south of equator descent and north of equator ascent (Figure 4h,f) but the enhancement in ascending motion extends only upto 15° N. ATL shows no significant circulation changes in the meridional plane (Figure 4e). The PAC is quite different than others that it shows ascent over a broader latitudinal band concentrated in upper levels above 500hPa and no enhanced descent is observed south of the equator over Indian longitudes, indicating a Walker circulation change (Figure 4g).

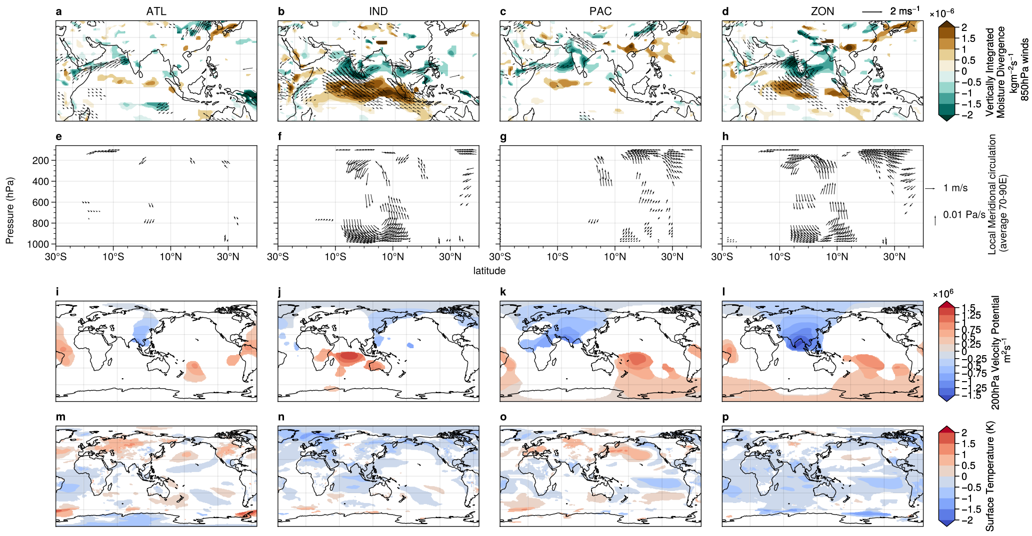

Figure 4. Circulation response: Response of (a-d) Vertically integrated moisture divergence between 1000-700hPa (shading) and 850hPa winds (vectors), (e-h) local meridional overturning circulation (average 70°-90°E) , (i-l) 200hPa velocity potential and (m-p) surface temperature in fully-coupled simulations for different experiments - (a,e,i,m) ATL, (b,f,j,n) IND, (c,g,k,o) PAC and (d,h,l,p) ZON for the climatology of simulation years 121-150. Only significant ($p < 0.05$) changes are shown in colour.

We confirm this by analysing the VP200 response of these experiments as proxy to the Walker circulation changes in the Indo-Pacific (Tanaka et al., 2004; Vecchi & Soden, 2007). For ZON and PAC, VP200 is reduced over the Asian continent (Figure 4k,l), reducing the existing positive bias. On the other hand, for IND, the main response is an increase in VP200 south of the equator over the Indian Ocean (Figure 4j) which adds to the existing positive bias (Figure 1b). For ZON and PAC we see a positive VP200 response in the Pacific Ocean south of the equator. Increases in VP200 in the Pacific and reduction over the Indian ocean are indications of a La Niña like Walker circulation response in these experiments. However existing strong negative VP200 biases in the north Pacific and the equatorial Atlantic remained same in all of the experiments (Figure 1b). The emergence of La Niña like conditions are further confirmed by the SST response, which shows cooling in the eastern equatorial Pacific in PAC and ZON (Figure 4o,p). This reduces the positive existing SST bias in this region (Figure 1c). In summary, the SASM changes in IND and ZON are brought about by changes in the meridional overturning circulation over Indian longitudes, but for PAC the driving mechanism is the zonal circulation change influenced by the equatorial Pacific SST. The ATL perturbation produces negligible changes in the large-scale circulation over South Asia. Reducing ASR biases over the subtropical Pacific modestly improve SASM precipitation biases over the Indian subcontinent. However, the key dynamic mechanism driving these improvements is not inter-hemispheric energy gradients, but instead zonal walker circulation changes caused the observed improvements. Our results imply that improving southern hemisphere subtropical radiation biases might improve SASM precipitation in climate models.

4 Discussion

In this study we investigated whether correcting an existing SH subtropical ASR bias in CESM2 will drive the ITCZ northwards and thereby correct the SASM precipitation biases during JJAS. Using CESM2 coupled simulations, we demonstrate that radiation biases in subtropical regions can indeed influence biases in simulations of regional monsoon precipitations. In general, when we correct SH subtropical ASR biases, global mean annual ITCZ shift northward following the energetic framework. Three of the experiments; IND, PAC and ZON; moved JJAS ITCZ northwards in the Indian Ocean reducing a southward bias. However these JJAS ITCZ corrections could not completely erase the SASM biases. The responses are regionally specific. An ASR correction in the ATL region has weak impacts on the SASM precipitation. Reducing the ASR bias over the subtropical southern Indian Ocean induces changes in meridional circulation over the SASM region and reduces precipitation in the equatorial Indian Ocean. In contrast reducing the bias over the subtropical south Pacific induces a La Niña-like temperature anomaly and circulation response thereby modestly increases the precipitation over the central land region of the SASM.

Our experiments suggest that the mean precipitation bias over the central land of the SASM region may be partially connected to the subtropical south Pacific radiation biases. It is interesting to see that a reduction in sunlight reaching the PAC can induce cooling in the equatorial Pacific and trigger a La Niña-like temperature and circulation response. However, the F_{TOA} corrections we applied here do not improve the biases in ocean regions surrounding South Asia; although the IND experiment hints to the meridional circulation anomalies that contribute to the dry bias south of equator in the Indian Ocean. Previous studies (Annamalai et al., 2017; He et al., 2022) have suggested that some of biases in oceanic precipitation can be explained by the local SST biases and errors in air-sea interactions over the northern Indian Ocean regions.

These results have implications for improvements in climate model monsoon fidelity, as we demonstrate that the SASM precipitation biases in CMIP6 climate models are influenced by the F_{TOA} radiation biases over subtropical southern hemisphere, particularly in the Indian and Pacific ocean basins (Figure S8). Given that a poor representation of marine stratocumulus clouds in climate models is the main cause of the ASR biases in subtropics (Jian et al., 2021), it is important to improve their representations in the climate models for better monsoon simulations. Coupled models used for seasonal prediction exhibit similar SASM biases i.e. dry bias over Indian land region and wet bias in surrounding oceanic region (Pillai et al., 2018). Major efforts are underway to understand and reduce these biases (e.g. Krishna et al. (2019); Fousiya et al. (2023)) and our findings indicate improvements in subtropical stratocumulus cloud biases may also provide improvements in seasonal prediction. Though here we presented results in context of the SASM precipitation only, other monsoon regions may see benefits from reducing low cloud biases. Notably, the Atlantic experiment shows reduction of the South American December-February precipitation biases over Brazil (Figures S2 and S7)

One important caveat of this work is that the sensitivity of southern subtropical radiation changes to SASM precipitation explained here could be different in different climate models. We performed experiments in only one model, CESM2, so the results should be interpreted cautiously, to account for CESM2 idiosyncrasies (like the high climate sensitivity (Gettelman et al., 2019) and large ENSO amplitude (Planton et al., 2021)). Despite this, our findings suggest that improving SH subtropical radiation biases may have the co-benefit of reducing SASM precipitation biases as well.

5 Open Research

CESM2 code modifications, model outputs and analysis scripts used to produce plots presented in the paper are available on Zenodo at `https://doi.org/10.5281/zenodo.10536019`.

Following are the freely available observation and climate model datasets used in the study - CMIP6 models used in this study are listed in Table S1 and the data is downloaded from the ESGF data portal (`https://esgf-node.llnl.gov/search/cmip6`) (Eyring et al., 2016), the ERA5 reanalysis data downloaded from the Copernicus Climate Data Store at `doi:10.24381/cds.6860a573` (Hersbach et al., 2020), CERES-EBAF version 4.2 data downloaded from `https://ceres.larc.nasa.gov/data/` (Loeb et al., 2018), the ERSST version 4 data downloaded from from their website at `doi:10.7289/V5KD1VVF` (Huang et al., 2015), and monthly GPCP precipitation version 2.3 data downloaded from National Centers for Environmental Information website `doi:10.7289/V56971M6` (Adler et al., 2018).

Acknowledgments
We thank Linda Hedges of SilverLining and Brian Dobbins of the National Center for Atmospheric Research for their valuable technical assistance with our CESM2 simulations. This work was partly funded by the DARPA AI-assisted Climate Tipping-point Modeling (ACTM) program under award DARPA-PA-21-04-02 and by an Natural Sciences and Engineering Research Council (NSERC) Alliance partnership grant ALLRP571068-21. The CESM2 simulations were performed using Amazon Web Services (AWS) thanks to a generous computing grant provided by Amazon.

References

Adler, R. F., Sapiano, M. R., Huffman, G. J., Wang, J.-J., Gu, G., Bolvin, D., ... others (2018). The global precipitation climatology project (gpcp) monthly analysis (new version 2.3) and a review of 2017 global precipitation. *Atmosphere*, *9*(4), 138.

Annamalai, H., Taguchi, B., McCreary, J. P., Nagura, M., & Miyama, T. (2017). Systematic errors in south asian monsoon simulation: Importance of equatorial indian ocean processes. *Journal of Climate*, *30*(20), 8159–8178.

Ashfaq, M., Rastogi, D., Mei, R., Touma, D., & Ruby Leung, L. (2017). Sources of errors in the simulation of south asian summer monsoon in the cmip5 gcms. *Climate Dynamics*, *49*, 193–223.

Atwood, A. R., Donohoe, A., Battisti, D. S., Liu, X., & Pausata, F. S. (2020). Robust longitudinally variable responses of the itcz to a myriad of climate forcings. *Geophysical Research Letters*, *47*(17), e2020GL088833.

Biasutti, M., Voigt, A., Boos, W. R., Braconnot, P., Hargreaves, J. C., Harrison, S. P., ... others (2018). Global energetics and local physics as drivers of past, present and future monsoons. *Nature Geoscience*, *11*(6), 392–400.

Bodas-Salcedo, A., Williams, K. D., Ringer, M. A., Beau, I., Cole, J. N., Dufresne, J.-L., ... Yokohata, T. (2014). Origins of the solar radiation biases over the southern ocean in cfmip2 models. *Journal of Climate*, *27*(1), 41–56.

Boos, W. R., & Hurley, J. V. (2013). Thermodynamic bias in the multimodel mean boreal summer monsoon. *Journal of climate*, *26*(7), 2279–2287.

Bordoni, S., & Schneider, T. (2008). Monsoons as eddy-mediated regime transitions of the tropical overturning circulation. *Nature Geoscience*, *1*(8), 515–519.

Choudhury, B. A., Rajesh, P., Zahan, Y., & Goswami, B. (2021). Evolution of the indian summer monsoon rainfall simulations from cmip3 to cmip6 models. *Climate Dynamics*, 1–26.

Danabasoglu, G., Lamarque, J.-F., Bacmeister, J., Bailey, D., DuVivier, A., Edwards, J., ... others (2020). The community earth system model version 2 (cesm2). *Journal of Advances in Modeling Earth Systems*, *12*(2), e2019MS001916.

Donohoe, A., Marshall, J., Ferreira, D., & Mcgee, D. (2013). The relationship between itcz location and cross-equatorial atmospheric heat transport: From the seasonal cycle to the last glacial maximum. *Journal of Climate*, *26*(11), 3597–3618.

Eyring, V., Bony, S., Meehl, G. A., Senior, C. A., Stevens, B., Stouffer, R. J., & Taylor, K. E. (2016). Overview of the coupled model intercomparison project phase 6 (cmip6) experimental design and organization. *Geoscientific Model Development*, *9*(5), 1937–1958.

Fousiya, T. S., Gnanaseelan, C., Halder, S., Kakatkar, R., Chowdary, J. S., Darshana, P., & Parekh, A. (2023). A new approach for seasonal prediction using the coupled model cfsv2 with special emphasis on indian summer monsoon. *International Journal of Climatology*, *43*(11), 4944-4964. Retrieved from `https://rmets.onlinelibrary.wiley.com/doi/abs/10.1002/joc.8126` doi: https://doi.org/10.1002/joc.8126

Frierson, D. M., & Hwang, Y.-T. (2012). Extratropical influence on itcz shifts in slab ocean simulations of global warming. *Journal of Climate*, *25*(2), 720–733.

Gadgil, S. (2018). The monsoon system: Land–sea breeze or the itcz? *Journal of Earth System Science*, *127*, 1–29.

Geen, R., Bordoni, S., Battisti, D. S., & Hui, K. (2020). Monsoons, itczs, and the concept of the global monsoon. *Reviews of Geophysics*, *58*(4), e2020RG000700.

Gettelman, A., Hannay, C., Bacmeister, J. T., Neale, R. B., Pendergrass, A., Danabasoglu, G., ... others (2019). High climate sensitivity in the community earth system model version 2 (cesm2). *Geophysical Research Letters*, *46*(14), 8329–8337.

Goswami, B., & Chakravorty, S. (2017). Dynamics of the indian summer monsoon climate. In *Oxford research encyclopedia of climate science.*

Gusain, A., Ghosh, S., & Karmakar, S. (2020). Added value of cmip6 over cmip5 models in simulating indian summer monsoon rainfall. *Atmospheric Research*, *232*, 104680.

Hanf, F. S., & Annamalai, H. (2020). Systematic errors in south asian monsoon precipitation: Process-based diagnostics and sensitivity to entrainment in ncar models. *Journal of Climate*, *33*(7), 2817–2840.

Hari, V., Villarini, G., Karmakar, S., Wilcox, L. J., & Collins, M. (2020). Northward propagation of the intertropical convergence zone and strengthening of indian summer monsoon rainfall. *Geophysical research letters*, *47*(23), e2020GL089823.

He, L., Zhou, T., & Chen, X. (2022). South asian summer rainfall from cmip3 to cmip6 models: biases and improvements. *Climate Dynamics*, 1–13.

Hersbach, H., Bell, B., Berrisford, P., Hirahara, S., Horányi, A., Muñoz-Sabater, J., ... others (2020). The era5 global reanalysis. *Quarterly Journal of the Royal Meteorological Society*, *146*(730), 1999–2049.

Hill, S. A. (2019). Theories for past and future monsoon rainfall changes. *Current Climate Change Reports*, *5*, 160–171.

Huang, B., Banzon, V. F., Freeman, E., Lawrimore, J., Liu, W., Peterson, T. C., ... Zhang, H.-M. (2015). Extended reconstructed sea surface temperature version 4 (ersst. v4). part i: Upgrades and intercomparisons. *Journal of climate*, *28*(3), 911–930.

Jain, S., Mishra, S. K., Anand, A., Salunke, P., & Fasullo, J. T. (2021). Historical and projected low-frequency variability in the somali jet and indian summer monsoon. *Climate Dynamics*, *56*, 749–765.

Jian, B., Li, J., Wang, G., Zhao, Y., Li, Y., Wang, J., ... Huang, J. (2021). Evaluation of the cmip6 marine subtropical stratocumulus cloud albedo and its controlling factors. *Atmospheric Chemistry and Physics*, *21*(12), 9809–9828.

Kang, S. M., Frierson, D. M., & Held, I. M. (2009). The tropical response to extratropical thermal forcing in an idealized gcm: The importance of radiative feedbacks and convective parameterization. *Journal of the atmospheric sciences*, *66*(9), 2812–2827.

Katzenberger, A., Schewe, J., Pongratz, J., & Levermann, A. (2021). Robust increase of indian monsoon rainfall and its variability under future warming in cmip6 models. *Earth System Dynamics*, *12*(2), 367–386.

Kay, J. E., Holland, M. M., Bitz, C. M., Blanchard-Wrigglesworth, E., Gettelman, A., Conley, A., & Bailey, D. (2012). The influence of local feedbacks and northward heat transport on the equilibrium arctic climate response to increased greenhouse gas forcing. *Journal of Climate*, *25*(16), 5433–5450.

Kim, H., Kang, S. M., Kay, J. E., & Xie, S.-P. (2022). Subtropical clouds key to southern ocean teleconnections to the tropical pacific. *Proceedings of the National Academy of Sciences*, *119*(34), e2200514119.

Konda, G., & Vissa, N. K. (2022). Evaluation of cmip6 models for simulations of surplus/deficit summer monsoon conditions over india. *Climate Dynamics*, 1–20.

Krishna, R. P. M., Rao, S. A., Srivastava, A., Kottu, H. P., Pradhan, M., Pillai, P., … Sabeerali, C. (2019). Impact of convective parameterization on the seasonal prediction skill of indian summer monsoon. *Climate Dynamics*, *53*, 6227–6243.

Kumar, T. L., Vinodhkumar, B., Rao, K. K., Chowdary, J., Osuri, K. K., & Desamsetti, S. (2023). Insights from the bias-corrected simulations of cmip6 in india's future climate. *Global and Planetary Change*, *226*, 104137.

Levine, R. C., Turner, A. G., Marathayil, D., & Martin, G. M. (2013). The role of northern arabian sea surface temperature biases in cmip5 model simulations and future projections of indian summer monsoon rainfall. *Climate dynamics*, *41*, 155–172.

Li, J.-L., Waliser, D., Stephens, G., Lee, S., L'Ecuyer, T., Kato, S., … Ma, H.-Y. (2013). Characterizing and understanding radiation budget biases in cmip3/cmip5 gcms, contemporary gcm, and reanalysis. *Journal of Geophysical Research: Atmospheres*, *118*(15), 8166–8184.

Li, J.-L., Xu, K.-M., Jiang, J., Lee, W.-L., Wang, L.-C., Yu, J.-Y., … Wang, Y.-H. (2020). An overview of cmip5 and cmip6 simulated cloud ice, radiation fields, surface wind stress, sea surface temperatures, and precipitation over tropical and subtropical oceans. *Journal of Geophysical Research: Atmospheres*, *125*(15), e2020JD032848.

Loeb, N. G., Doelling, D. R., Wang, H., Su, W., Nguyen, C., Corbett, J. G., … Kato, S. (2018). Clouds and the earth's radiant energy system (ceres) energy balanced and filled (ebaf) top-of-atmosphere (toa) edition-4.0 data product. *Journal of Climate*, *31*(2), 895–918.

Mitra, A. (2021). A comparative study on the skill of cmip6 models to preserve daily spatial patterns of monsoon rainfall over india. *Frontiers in Climate*, *3*, 654763.

Pillai, P. A., Rao, S. A., Ramu, D. A., Pradhan, M., & George, G. (2018). Seasonal prediction skill of indian summer monsoon rainfall in nmme models and monsoon mission cfsv2. *International Journal of Climatology*, *38*, e847–e861.

Planton, Y. Y., Guilyardi, E., Wittenberg, A. T., Lee, J., Gleckler, P. J., Bayr, T., … others (2021). Evaluating climate models with the clivar 2020 enso metrics package. *Bulletin of the American Meteorological Society*, *102*(2), E193–E217.

Rajendran, K., Surendran, S., Varghese, S. J., & Sathyanath, A. (2022). Simulation of indian summer monsoon rainfall, interannual variability and teleconnections: evaluation of cmip6 models. *Climate Dynamics*, *58*(9-10), 2693–2723.

Schneider, T., Bischoff, T., & Haug, G. H. (2014). Migrations and dynamics of the intertropical convergence zone. *Nature*, *513*(7516), 45–53.

Tanaka, H. L., Ishizaki, N., & Kitoh, A. (2004). Trend and interannual variability of walker, monsoon and hadley circulations defined by velocity potential in the upper troposphere. *Tellus A: Dynamic Meteorology and Oceanography*, *56*(3), 250–269.

Vecchi, G. A., & Soden, B. J. (2007). Global warming and the weakening of the tropical circulation. *Journal of Climate*, *20*(17), 4316–4340.

Voigt, A., Biasutti, M., Scheff, J., Bader, J., Bordoni, S., Codron, F., ... others (2016). The tropical rain belts with an annual cycle and a continent model intercomparison project: Tracmip. *Journal of Advances in Modeling Earth Systems*, *8*(4), 1868–1891.

Walker, G. (1923). Correlation in seasonal variations of weather, viii: A preliminary study of weather. *Mem. Indian Meteor. Dep*, *24*, 75–131.

Xiang, B., Zhao, M., Ming, Y., Yu, W., & Kang, S. M. (2018). Contrasting impacts of radiative forcing in the southern ocean versus southern tropics on itcz position and energy transport in one gfdl climate model. *Journal of Climate*, *31*(14), 5609–5628.

Xiao, H., Mechoso, C. R., Sun, R., Han, J., Pan, H.-L., Park, S., ... Teixeira, J. (2014). Diagnosis of the marine low cloud simulation in the ncar community earth system model (cesm) and the ncep global forecast system (gfs)-modular ocean model v4 (mom4) coupled model. *Climate dynamics*, *43*, 737–752.

Zhao, L., Wang, Y., Zhao, C., Dong, X., & Yung, Y. L. (2022). Compensating errors in cloud radiative and physical properties over the southern ocean in the cmip6 climate models. *Advances in Atmospheric Sciences*, *39*(12), 2156–2171.

South Asian Summer Monsoon Precipitation is Sensitive to Southern Hemisphere Subtropical Radiation Changes

Dipti Hingmire[1], Haruki Hirasawa[1], Hansi Singh[1,5], Philip J. Rasch[2], Sookyung Kim[3,6], Subhashis Hazarika[3,6], Peetak Mitra[3,4], Kalai Ramea[3,5]

[1]School of Earth and Ocean Sciences, University of Victoria, Victoria, BC, Canada
[2]Department of Atmospheric Sciences, University of Washington, Seattle, WA, USA
[3]Palo Alto Research Corporation, Palo Alto, CA, USA
[4]Excarta, Palo Alto, CA, USA
[5]Planette Inc., San Francisco, CA, USA
[6]SRI International, Palo Alto, CA, USA

Key Points:

- We test if biases in southern hemisphere shortwave radiation contributes to biases in South Asian Summer Monsoon Precipitation in the CESM2.
- Reducing incoming shortwave radiation in the subtropical southern hemisphere reduces dry biases over continental South Asia.
- This effect is mostly due to forcing in the South Pacific, with less impact from the Atlantic or Indian ocean.

Corresponding author: Dipti Hingmire, `dhingmire@uvic.ca`

Abstract

We study the sensitivity of South Asian Summer Monsoon (SASM) precipitation to Southern Hemisphere (SH) subtropical Absorbed Solar Radiation (ASR) changes using Community Earth System Model 2 simulations. Reducing positive ASR biases over the SH subtropics impacts SASM, and is sensitive to the ocean basin where changes are imposed. Radiation changes over the SH subtropical Indian Ocean (IO) shifts rainfall over the equatorial IO northward causing 1-2 mm/day drying south of equator, changes over the SH subtropical Pacific increases precipitation over northern continental regions by 1-2 mm/day, and changes over the SH subtropical Atlantic have little effect on SASM precipitation. Radiation changes over the subtropical Pacific impacts the SASM through zonal circulation changes, while changes over the IO modify meridional circulation to bring about changes in precipitation over northern IO. Our findings suggest that reducing SH subtropical radiation biases in climate models may also reduce SASM precipitation biases.

Plain Language Summary

Precipitation from South Asian Summer Monsoon (SASM) is of high significance to the livelihoods of over a billion people. As the global climate continues to evolve, it is essential to have a clear understanding of the possible future changes to the SASM. However, current state-of-the-art climate models have difficulties in simulating climatological mean SASM precipitations. Here we study sensitivity of SASM precipitation to subtropical southern ocean radiation as one of the possible causes of SASM precipitation bias. Our experiments indicate that SASM precipitation is sensitive to southern hemisphere subtropical radiation changes particularly to those in subtropical Pacific. These findings imply that improving southern hemisphere subtropical radiation biases might improve SASM precipitation simulations in climate models.

1 Introduction

The South Asian Summer Monsoon (SASM) is a highly influential monsoon system, known for its strength, spatial extent, and significance to the livelihoods of over a billion people. Future greenhouse gas forcing is projected to increase SASM precipitation, but the magnitude and pattern of these changes remain uncertain (Katzenberger et al., 2021; Kumar et al., 2023). Earth System Models (ESMs) serve as the primary means of projecting these changes, but ESMs have long-standing biases in simulating the SASM's climatological precipitation intensity, spatial pattern, and seasonality, among other elements (Mitra, 2021; Konda & Vissa, 2022; Rajendran et al., 2022). These biases have been attributed to various sources, including errors in representation of orography (Boos & Hurley, 2013), land-atmosphere interactions (Ashfaq et al., 2017), air-sea interactions (Annamalai et al., 2017; Hanf & Annamalai, 2020), and sea surface temperatures over the Indian Ocean (Levine et al., 2013; He et al., 2022). ESMs participating in the Coupled Model Intercomparison Project 6 (CMIP6) better simulate the SASM compared to previous generations of models, but significant biases persist (Gusain et al., 2020; Choudhury et al., 2021).

The Community Earth System Model 2 (CESM2) (Danabasoglu et al., 2020), like other climate models, has systematic biases in simulating SASM precipitation. Figure 1a displays the June to September (JJAS) precipitation and lower tropospheric circulation biases for the 1979-2014 period compared to observations and reanalysis. CESM2 does not produce enough precipitation in two regions of the SASM system: (1) over the central land region between 20°-30°N, and (2) over the Indian Ocean between 10°S-0°N with dry biases of 2-4 mm/day over both regions. Between these two dry biased areas, there is a region of excessive precipitation (4-6 mm/day) in the northern Indian ocean surrounding the South Asian landmass producing a meridional dry-wet-dry bias pattern.

The model also tends to overestimate precipitation over the high orography of the Eastern Himalayas, Southeast Asia, and the Maritime continent.

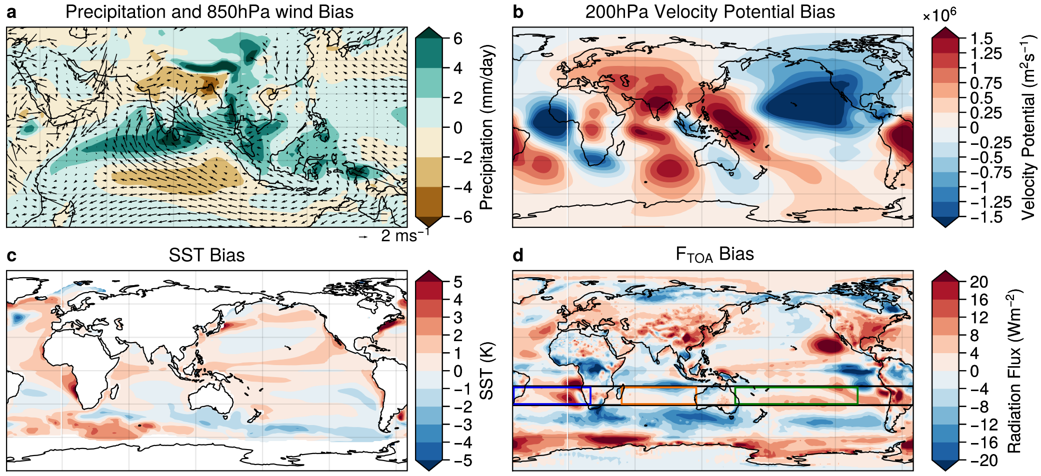

Figure 1. Existing biases in CESM2: Ensemble mean bias of 11 members of CESM2 historical simulations from CMIP dataset in (a) JJAS precipitation, and 850 hPa wind with respect to GPCP (Adler et al., 2018) and ERA5 (Hersbach et al., 2020), respectively; (b) JJAS 200 hPa velocity potential relative to ERA5; and (c) annual mean SST relative to ERSST (Huang et al., 2015); and (d) annual mean net downward top-of-atmosphere (F_{TOA}) radiation flux relative to CERES-EBAF (Loeb et al., 2018). Biases are calculated based on climatology of period 2004-2014 for F_{TOA} and 1979-2014 for all other variables. Boxes in panel d show the specific region where CDNC perturbations are applied for Atlantic (ATL, blue), Indian Ocean (IND, orange), Pacific (PAC, green) and Zonal (ZON, black) experiments.

SASM biases are linked to biases in the regional circulation, which partly arise from local Sea Surface Temperature (SST) biases (Annamalai et al., 2017; He et al., 2022). In CESM2, lower tropospheric winds are biased southeasterly and southerly over the equatorial Indian ocean and parts of Arabian Sea (Figure 1a) and are biased northwesterly over Indian land regions and the Bay of Bengal. Figure 1b displays the upper troposphere circulation bias in terms of the 200hPa velocity potential (VP200). The VP200 bias is greatest over the land regions of India and south of the equator up to 10°S. These positive VP200 biases correspond to subsidence and weaker convergence at lower tropospheric levels, thereby creating dry biases. CESM2 also displays positive SST biases in the tropics globally, which affects the Walker circulation and thus the SASM (Walker, 1923; Jain et al., 2021).

An emerging view is that regional tropical monsoons are local manifestations of seasonal Intertropical Convergence Zone (ITCZ) shifts, and are an important feature of an energy-constrained global circulation (Bordoni & Schneider, 2008; Biasutti et al., 2018; Hill, 2019; Geen et al., 2020). SASM variability in particular is strongly linked to seasonal migrations of the ITCZ over the Indian subcontinent (Gadgil, 2018; Hari et al., 2020). These seasonal ITCZ migrations are in turn driven by inter-hemispheric energy gradients, as the Hadley circulation, and thus the ITCZ shift, towards the warmer hemisphere to transport excess energy to the opposite hemisphere (Kang et al., 2009; Schneider et al., 2014). Thus, a systematic Absorbed Solar Radiation (ASR) bias could alter this inter-hemispheric energy gradient, thereby disrupting this seasonal ITCZ migration and inducing biases in the monsoon. While ASR biases over the Southern Ocean have been reduced in the latest generation of climate models (Kay et al., 2012; Bodas-Salcedo et al., 2014; Zhao et al., 2022), positive radiation biases still exist over the subtropical Southern Hemisphere (SH) oceans in many ESMs (Li et al., 2013, 2020). In CESM2, the midlatitude SH displays a negative net downward top-of-atmosphere (F_{TOA}) radiation bias while the subtropical SH has a positive F_{TOA} bias between 15°-30°S (Figure 1d), which may be due to insufficient low cloud cover (Xiao et al., 2014) and too weak stratocumulus cloud feedbacks (Kim et al., 2022). This positive SH subtropical F_{TOA} bias is greatest over the Atlantic and Pacific Oceans, but is relatively small in the Indian Ocean.

In the present study, we aim to address the following: does improving SH subtropical radiation biases impact ITCZ position and the simulation of the SASM? And if so, by what mechanism? To test this, we perform CESM2 experiments where we decrease ASR in SH regions with high ASR biases by changing the cloud albedo. We change the cloud properties by prescribing the Cloud Droplet Number Concentration (CDNC) that influences the cloud microphysics and radiation. Our results indicate that reducing ASR biases over the subtropical SH modestly improve SASM precipitation biases over the Indian subcontinent.

2 Methods

To understand the effect of reducing SH ASR biases on SASM, we performed a series of experiments with the Community Earth System model 2 (CESM2, Danabasoglu et al., 2020), the latest generation ESM developed by the National Center for Atmospheric Research and collaborators. Our configuration uses CAM6 for atmosphere, POP2 for ocean, CLM5 for land and CICE5 for sea ice. In our experiments, we perturbed the radiative fluxes in CESM2 by prescribing the in-cloud liquid CDNC at all vertical levels where liquid and mixed phase clouds exist over oceanic regions in the SH subtropics. This reduces the average cloud droplet radius, increasing cloud albedo and lifetime, and thus reducing ASR.

First we conducted Fixed Sea Surface Temperature (Fixed-SST) experiments to identify the sensitivity of F_{TOA} fluxes to CDNC, and determined the CDNC values that would minimize the ASR bias compared to observations. We then carried out five fully coupled simulations with repeating year-2000 forcings - one control simulation (2000CNT) without any perturbations and four experiments which introduced the identified CDNC perturbations in different regions of SH subtropics (15°-30°S) (listed in Table 1). The first three simulations introduced a perturbation in each of the Atlantic (ATL) [50°W-20°E], Indian (IND) [48°-115°E], and Pacific (PAC) [150°E-80°W] oceans and the fourth simulation perturbed ocean regions in the entire zonal band (ZON) (180°W-180°E). We set the CDNC value to 150 cm^{-3} for ATL and 75 cm^{-3} for the PAC, IND, and ZON experiments. When compared to existing CESM2 F_{TOA} bias with EBAF (Figure 1d), the applied perturbations correct most of the F_{TOA} bias in the subtropical SH Atlantic but over the subtropical SH Pacific and Indian Ocean the perturbation exceeds F_{TOA} bias, resulting in a negative bias (Figure S1 and Table 1). Fixed-SST experiments were run for 7 years and fully coupled experiments for 150 years. We calculate the response as the climatological average difference between perturbation experiment and control run for the last 5 and 30 years of the fixed-SST and fully coupled simulations respectively. Statistical significance of response is tested using the Student's t-test with $p < 0.05$.

2.1 ITCZ position

We compute the ITCZ latitude as the centroid of the zonal-mean, time-mean precipitation between 30°N and 30°S (Frierson & Hwang, 2012; Voigt et al., 2016). As demonstrated by Atwood et al. (2020), regional rainbelts do not shift uniformly in response to hemispherically asymmetric forcing, therefore we also analyse regional ITCZs in the Atlantic (10°W–40°W), Indian (70°E -90°E) and Pacific (110°E–100°W) oceans.

Table 1. Details of coupled CESM2 experiments used in this study

Experiment name	Abbreviation	CDNC perturbation applied	Perturbation Region	Global F_{TOA} response in W/m2	Regional F_{TOA} response in W/m2 (Existing CESM2 bias)
Control	2000CNT	0	0	0	0
Atlantic	ATL	150 cm^{-3}	50°W-20°E, 15°-30°S	-0.21±0.87	-5.43 ±1.28 (5.77 ±0.19)
Indian Ocean	IND	75 cm^{-3}	48°-115°E, 15°-30°S	-0.08±0.88	-5.71 ±1.5 (-2.50 ±0.2)
Pacific	PAC	75 cm^{-3}	150°E-80°W, 15°-30°S	-0.39 ±0.85	-7.27 ±1.21 (3.31 ±0.3)
Zonal	ZON	75 cm^{-3}	180°W-180°E, 15°-30°S	-0.53±0.88	-4.34 ±1.23 (2.43 ±0.23)

3 Results

3.1 Energetically constrained global precipitation response

All experiments show energy being transported towards the SH subtropics, where we created an ASR depression by artificially increasing CDNC, producing increasing northward transport between 60-30 S (positive values) and southward transport between 15S-30N (negative values) (Figure 2a). The experiments show similar responses in terms of direction of transport however the magnitude of response differs. The magnitude is proportional to the F_{TOA} anomaly e.g. ZON shows highest absolute F_{TOA} and total energy transport response while as IND shows least absolute values for the both (See Table 1 and Figure 2a). Most of this energy transport is carried out by atmospheric transport as shown by Atmospheric Energy Transport (AET) response in Figure 2b. Experiments show varied ocean heat transport responses but the changes are one order less than that of AET (Figure 2c). These results confirm the findings of Xiang et al. (2018) that atmosphere transports energy more effectively than oceans when energy perturbations are applied at lower latitudes.

Following the energetics framework (Kang et al., 2009; Schneider et al., 2014; Donohoe et al., 2013), AET changes bring about changes in precipitations as shown in Figure 2d. All the experiments show increase of precipitation in the tropical northern hemisphere and reductions in the tropical SH, indicating northward migration of the ITCZ. Consistent with AET response, the precipitation change is larger in ZON and PAC and weaker in IND and ATL. In Figure 2e and 2f, we quantify these ITCZ shifts and their biases. In CESM2, the annual mean ITCZ position has northward bias of 0.25 ° (Figure 2e). However, this bias is regionally and seasonally dependent. In the context of the SASM we are interested in JJAS ITCZ location in Indian Ocean, which is biased 1.2° southwards (Figure 2f). All of the experiments show significant northward shifts in respective regional annual and JJAS global ITCZs (Figure 2e and 2f). Notably, IND, PAC and ZON show significant northward shifts in annual and JJAS mean ITCZ over the Indian Ocean. Thus, as hypothesized, our experiments show that the ITCZ responses followed the energetic framework.

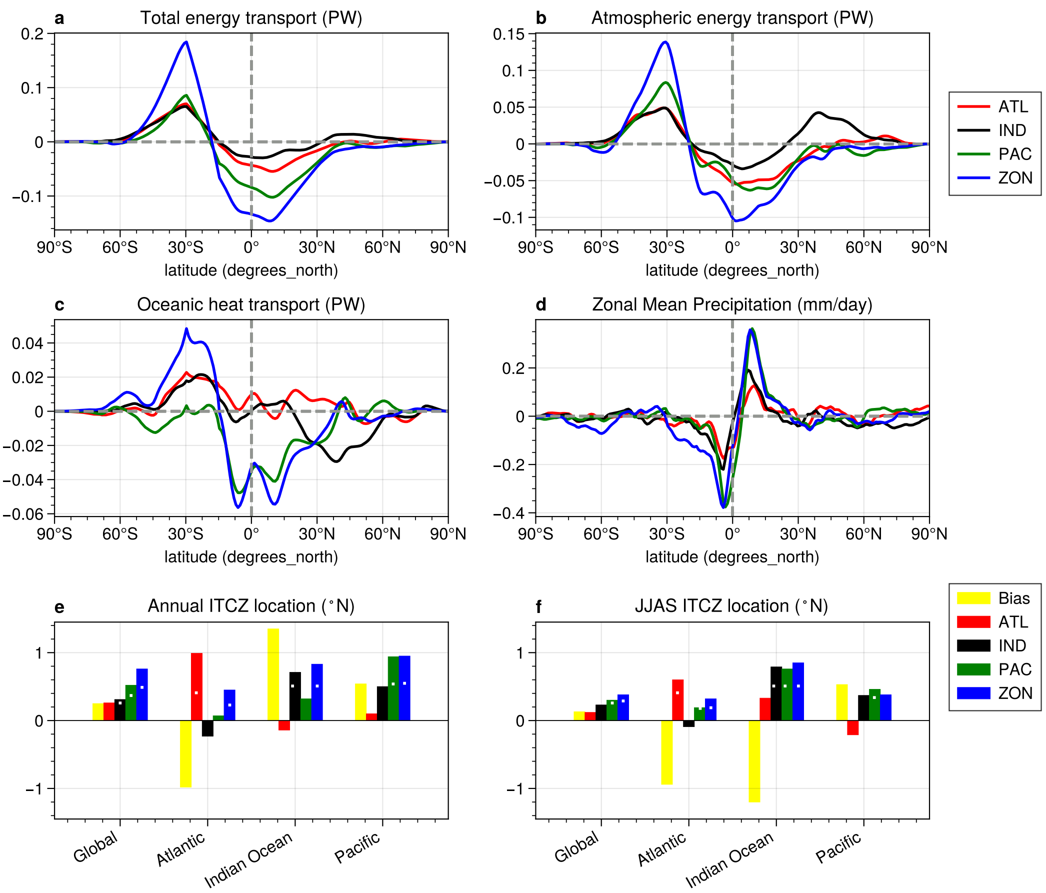

Figure 2. Global energetic and precipitation response: Zonal mean response of (a) total energy tranport, (b) atmospheric energy transport, (c) ocean heat transport, (d) annual mean precipitation, (e) annual and (f) JJAS ITCZ position shift in fully coupled simulation for ATL (red), IND (black), PAC (green) and ZON (blue) experiments and CESM2 existing biases (yellow in e and f panels). White dots in panels e and f indicate the statistically significant shifts of ITCZ.

3.2 SASM precipitation response

We now consider how the ITCZ shifts influence SASM precipitation. Despite the similar effect of IND, PAC and ZON on the JJAS Indian Ocean ITCZ, the SASM precipitation response differ considerably in these experiments (Figure 3). Reducing ASR in the PAC causes significant precipitation increases over the central continental India. This stands out from the other experiments and contributes to a reduction of the JJAS dry bias over this region (Figure 3c; see Figure 1a for bias). However, the increase in precipitation of 1-2 mm/day for the PAC is only a partial compensation for the 2-4 mm/day dry bias of SASM precipitation in CESM2 over this region. For the ATL experiment, whose main ITCZ response is in the Atlantic, the JJAS SASM precipitation change is largely non-significant over the SASM region (Figure 3a). It is also interesting to see that IND experiment moves the annual and JJAS ITCZ northwards (Figure 2e and 2f) and produces precipitation decrease of 1-2 mm/day (Figure 3b) south of equator thus adding to JJAS SASM dry bias over there (Figure 1a). The ZON experiment is similar to IND experiment: significant precipitation increase of 1-2mm/day add to existing wet bias over oceanic regions surrounding Indian land and precipitation decrease of 1mm/day add to

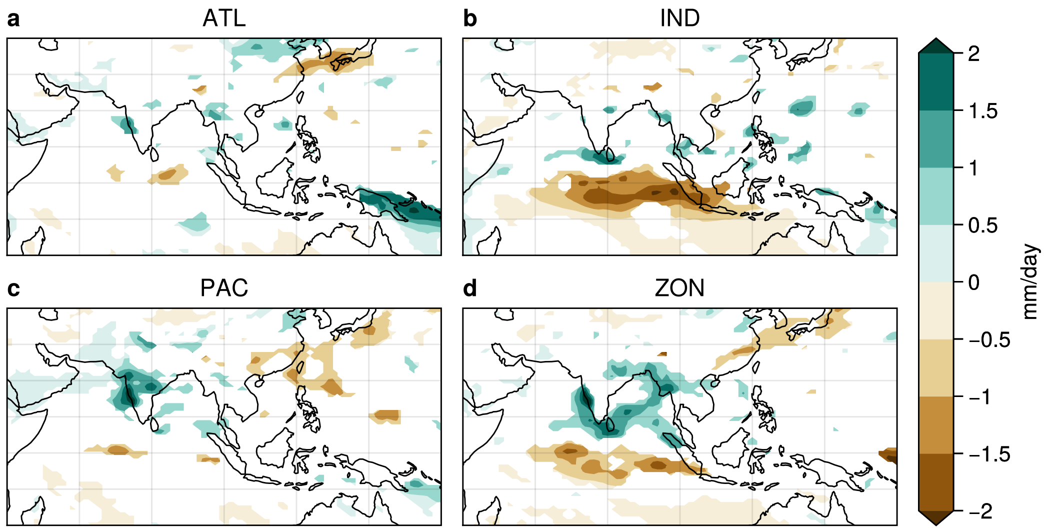

Figure 3. SASM precipitation response: JJAS precipitation response (at simulation period 121-150 years) in fully coupled simulation for experiments (a) ATL, (b) IND, (c) PAC and (d) ZON. Non-significant responses (at level of significance 0.05) are masked in white.

dry biases (Figure 3d) south of the equator. It also reduces dry bias of a small portion over central India east of 80°E. To better decipher these intriguing SASM precipitation responses in different experiments we further explore the large-scale circulation changes in each of these experiments.

3.3 Large-scale circulation response

Panels a-d in Figure 4 show lower tropospheric circulation and associated moisture divergence for each of the experiments. For IND and ZON, the 850hPa wind responses add to existing southeasterly and southerly biases in the equatorial Indian Ocean and parts of the Arabian sea (Figure 4b and d, see Figure 1a for bias). The important wind response of PAC is a southeasterly response over land regions of central India (Figure 4c) which reduces northwesterly circulation bias (Figure 1a). In tandem with lower tropospheric circulation changes, we observe that moisture convergence increases over Indian land region for PAC but over the surrounding oceanic regions for ZON and IND (Figure 4b,c and d). The ATL shows statistically significant increase in lower tropospheric westerlies and the moisture convergence along the west coast (Figure 4a) over a small region. The improved representation of lower level winds and increased moisture flux convergence over central continental India in PAC, contributes to a partial reduction of the dry precipitation bias over this region.

The SASM regional circulation is tightly linked to the large-scale Hadley circulation in the meridional plane and the Walker circulation in the zonal plane (Goswami & Chakravorty, 2017). ZON and IND, show strengthening of the meridional overturning circulation with enhanced south of equator descent and north of equator ascent (Figure 4h,f) but the enhancement in ascending motion extends only upto 15° N. ATL shows no significant circulation changes in the meridional plane (Figure 4e). The PAC is quite different than others that it shows ascent over a broader latitudinal band concentrated in upper levels above 500hPa and no enhanced descent is observed south of the equator over Indian longitudes, indicating a Walker circulation change (Figure 4g).

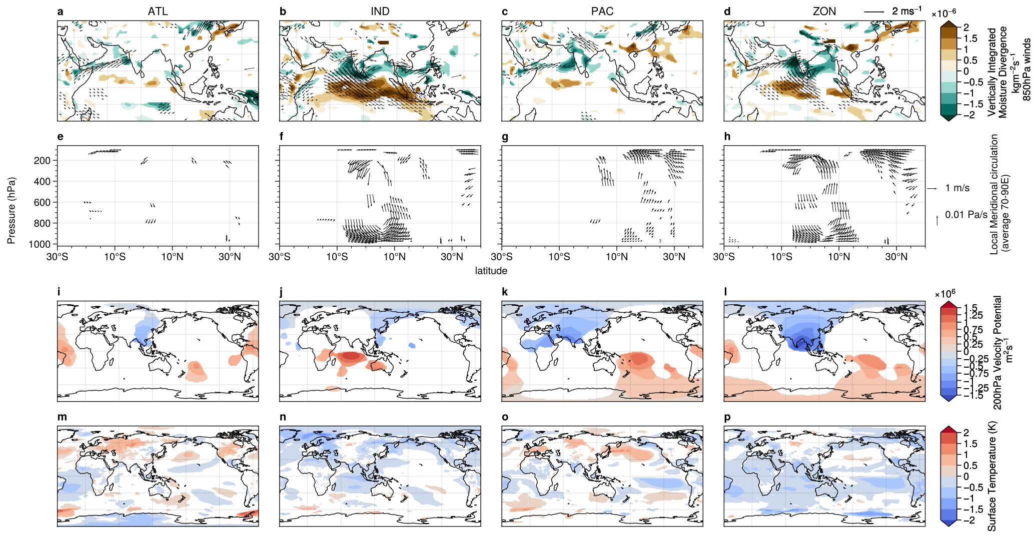

Figure 4. Circulation response: Response of (a-d) Vertically integrated moisture divergence between 1000-700hPa (shading) and 850hPa winds (vectors), (e-h) local meridional overturning circulation (average 70°-90°E) , (i-l) 200hPa velocity potential and (m-p) surface temperature in fully-coupled simulations for different experiments - (a,e,i,m) ATL, (b,f,j,n) IND, (c,g,k,o) PAC and (d,h,l,p) ZON for the climatology of simulation years 121-150. Only significant ($p < 0.05$) changes are shown in colour.

We confirm this by analysing the VP200 response of these experiments as proxy to the Walker circulation changes in the Indo-Pacific (Tanaka et al., 2004; Vecchi & Soden, 2007). For ZON and PAC, VP200 is reduced over the Asian continent (Figure 4k,l), reducing the existing positive bias. On the other hand, for IND, the main response is an increase in VP200 south of the equator over the Indian Ocean (Figure 4j) which adds to the existing positive bias (Figure 1b). For ZON and PAC we see a positive VP200 response in the Pacific Ocean south of the equator. Increases in VP200 in the Pacific and reduction over the Indian ocean are indications of a La Niña like Walker circulation response in these experiments. However existing strong negative VP200 biases in the north Pacific and the equatorial Atlantic remained same in all of the experiments (Figure 1b). The emergence of La Niña like conditions are further confirmed by the SST response, which shows cooling in the eastern equatorial Pacific in PAC and ZON (Figure 4o,p). This reduces the positive existing SST bias in this region (Figure 1c). In summary, the SASM changes in IND and ZON are brought about by changes in the meridional overturning circulation over Indian longitudes, but for PAC the driving mechanism is the zonal circulation change influenced by the equatorial Pacific SST. The ATL perturbation produces negligible changes in the large-scale circulation over South Asia. Reducing ASR biases over the subtropical Pacific modestly improve SASM precipitation biases over the Indian subcontinent. However, the key dynamic mechanism driving these improvements is not inter-hemispheric energy gradients, but instead zonal walker circulation changes caused the observed improvements. Our results imply that improving southern hemisphere subtropical radiation biases might improve SASM precipitation in climate models.

4 Discussion

In this study we investigated whether correcting an existing SH subtropical ASR bias in CESM2 will drive the ITCZ northwards and thereby correct the SASM precipitation biases during JJAS. Using CESM2 coupled simulations, we demonstrate that radiation biases in subtropical regions can indeed influence biases in simulations of regional monsoon precipitations. In general, when we correct SH subtropical ASR biases, global mean annual ITCZ shift northward following the energetic framework. Three of the experiments; IND, PAC and ZON; moved JJAS ITCZ northwards in the Indian Ocean reducing a southward bias. However these JJAS ITCZ corrections could not completely erase the SASM biases. The responses are regionally specific. An ASR correction in the ATL region has weak impacts on the SASM precipitation. Reducing the ASR bias over the subtropical southern Indian Ocean induces changes in meridional circulation over the SASM region and reduces precipitation in the equatorial Indian Ocean. In contrast reducing the bias over the subtropical south Pacific induces a La Niña-like temperature anomaly and circulation response thereby modestly increases the precipitation over the central land region of the SASM.

Our experiments suggest that the mean precipitation bias over the central land of the SASM region may be partially connected to the subtropical south Pacific radiation biases. It is interesting to see that a reduction in sunlight reaching the PAC can induce cooling in the equatorial Pacific and trigger a La Niña-like temperature and circulation response. However, the F_{TOA} corrections we applied here do not improve the biases in ocean regions surrounding South Asia; although the IND experiment hints to the meridional circulation anomalies that contribute to the dry bias south of equator in the Indian Ocean. Previous studies (Annamalai et al., 2017; He et al., 2022) have suggested that some of biases in oceanic precipitation can be explained by the local SST biases and errors in air-sea interactions over the northern Indian Ocean regions.

These results have implications for improvements in climate model monsoon fidelity, as we demonstrate that the SASM precipitation biases in CMIP6 climate models are influenced by the F_{TOA} radiation biases over subtropical southern hemisphere, particularly in the Indian and Pacific ocean basins (Figure S8). Given that a poor representation of marine stratocumulus clouds in climate models is the main cause of the ASR biases in subtropics (Jian et al., 2021), it is important to improve their representations in the climate models for better monsoon simulations. Coupled models used for seasonal prediction exhibit similar SASM biases i.e. dry bias over Indian land region and wet bias in surrounding oceanic region (Pillai et al., 2018). Major efforts are underway to understand and reduce these biases (e.g. Krishna et al. (2019); Fousiya et al. (2023)) and our findings indicate improvements in subtropical stratocumulus cloud biases may also provide improvements in seasonal prediction. Though here we presented results in context of the SASM precipitation only, other monsoon regions may see benefits from reducing low cloud biases. Notably, the Atlantic experiment shows reduction of the South American December-February precipitation biases over Brazil (Figures S2 and S7)

One important caveat of this work is that the sensitivity of southern subtropical radiation changes to SASM precipitation explained here could be different in different climate models. We performed experiments in only one model, CESM2, so the results should be interpreted cautiously, to account for CESM2 idiosyncrasies (like the high climate sensitivity (Gettelman et al., 2019) and large ENSO amplitude (Planton et al., 2021)). Despite this, our findings suggest that improving SH subtropical radiation biases may have the co-benefit of reducing SASM precipitation biases as well.

5 Open Research

CESM2 code modifications, model outputs and analysis scripts used to produce plots presented in the paper are available on Zenodo at `https://doi.org/10.5281/zenodo.10536019`.

Following are the freely available observation and climate model datasets used in the study - CMIP6 models used in this study are listed in Table S1 and the data is downloaded from the ESGF data portal (`https://esgf-node.llnl.gov/search/cmip6`) (Eyring et al., 2016), the ERA5 reanalysis data downloaded from the Copernicus Climate Data Store at `doi:10.24381/cds.6860a573` (Hersbach et al., 2020), CERES-EBAF version 4.2 data downloaded from `https://ceres.larc.nasa.gov/data/` (Loeb et al., 2018), the ERSST version 4 data downloaded from from their website at `doi:10.7289/V5KD1VVF` (Huang et al., 2015), and monthly GPCP precipitation version 2.3 data downloaded from National Centers for Environmental Information website `doi:10.7289/V56971M6` (Adler et al., 2018).

Acknowledgments

We thank Linda Hedges of SilverLining and Brian Dobbins of the National Center for Atmospheric Research for their valuable technical assistance with our CESM2 simulations. This work was partly funded by the DARPA AI-assisted Climate Tipping-point Modeling (ACTM) program under award DARPA-PA-21-04-02 and by an Natural Sciences and Engineering Research Council (NSERC) Alliance partnership grant ALLRP571068-21. The CESM2 simulations were performed using Amazon Web Services (AWS) thanks to a generous computing grant provided by Amazon.

References

Adler, R. F., Sapiano, M. R., Huffman, G. J., Wang, J.-J., Gu, G., Bolvin, D., … others (2018). The global precipitation climatology project (gpcp) monthly analysis (new version 2.3) and a review of 2017 global precipitation. *Atmosphere*, *9*(4), 138.

Annamalai, H., Taguchi, B., McCreary, J. P., Nagura, M., & Miyama, T. (2017). Systematic errors in south asian monsoon simulation: Importance of equatorial indian ocean processes. *Journal of Climate*, *30*(20), 8159–8178.

Ashfaq, M., Rastogi, D., Mei, R., Touma, D., & Ruby Leung, L. (2017). Sources of errors in the simulation of south asian summer monsoon in the cmip5 gcms. *Climate Dynamics*, *49*, 193–223.

Atwood, A. R., Donohoe, A., Battisti, D. S., Liu, X., & Pausata, F. S. (2020). Robust longitudinally variable responses of the itcz to a myriad of climate forcings. *Geophysical Research Letters*, *47*(17), e2020GL088833.

Biasutti, M., Voigt, A., Boos, W. R., Braconnot, P., Hargreaves, J. C., Harrison, S. P., … others (2018). Global energetics and local physics as drivers of past, present and future monsoons. *Nature Geoscience*, *11*(6), 392–400.

Bodas-Salcedo, A., Williams, K. D., Ringer, M. A., Beau, I., Cole, J. N., Dufresne, J.-L., … Yokohata, T. (2014). Origins of the solar radiation biases over the southern ocean in cfmip2 models. *Journal of Climate*, *27*(1), 41–56.

Boos, W. R., & Hurley, J. V. (2013). Thermodynamic bias in the multimodel mean boreal summer monsoon. *Journal of climate*, *26*(7), 2279–2287.

Bordoni, S., & Schneider, T. (2008). Monsoons as eddy-mediated regime transitions of the tropical overturning circulation. *Nature Geoscience*, *1*(8), 515–519.

Choudhury, B. A., Rajesh, P., Zahan, Y., & Goswami, B. (2021). Evolution of the indian summer monsoon rainfall simulations from cmip3 to cmip6 models. *Climate Dynamics*, 1–26.

Danabasoglu, G., Lamarque, J.-F., Bacmeister, J., Bailey, D., DuVivier, A., Edwards, J., ... others (2020). The community earth system model version 2 (cesm2). *Journal of Advances in Modeling Earth Systems*, *12*(2), e2019MS001916.

Donohoe, A., Marshall, J., Ferreira, D., & Mcgee, D. (2013). The relationship between itcz location and cross-equatorial atmospheric heat transport: From the seasonal cycle to the last glacial maximum. *Journal of Climate*, *26*(11), 3597–3618.

Eyring, V., Bony, S., Meehl, G. A., Senior, C. A., Stevens, B., Stouffer, R. J., & Taylor, K. E. (2016). Overview of the coupled model intercomparison project phase 6 (cmip6) experimental design and organization. *Geoscientific Model Development*, *9*(5), 1937–1958.

Fousiya, T. S., Gnanaseelan, C., Halder, S., Kakatkar, R., Chowdary, J. S., Darshana, P., & Parekh, A. (2023). A new approach for seasonal prediction using the coupled model cfsv2 with special emphasis on indian summer monsoon. *International Journal of Climatology*, *43*(11), 4944-4964. Retrieved from https://rmets.onlinelibrary.wiley.com/doi/abs/10.1002/joc.8126 doi: https://doi.org/10.1002/joc.8126

Frierson, D. M., & Hwang, Y.-T. (2012). Extratropical influence on itcz shifts in slab ocean simulations of global warming. *Journal of Climate*, *25*(2), 720–733.

Gadgil, S. (2018). The monsoon system: Land–sea breeze or the itcz? *Journal of Earth System Science*, *127*, 1–29.

Geen, R., Bordoni, S., Battisti, D. S., & Hui, K. (2020). Monsoons, itczs, and the concept of the global monsoon. *Reviews of Geophysics*, *58*(4), e2020RG000700.

Gettelman, A., Hannay, C., Bacmeister, J. T., Neale, R. B., Pendergrass, A., Danabasoglu, G., ... others (2019). High climate sensitivity in the community earth system model version 2 (cesm2). *Geophysical Research Letters*, *46*(14), 8329–8337.

Goswami, B., & Chakravorty, S. (2017). Dynamics of the indian summer monsoon climate. In *Oxford research encyclopedia of climate science.*

Gusain, A., Ghosh, S., & Karmakar, S. (2020). Added value of cmip6 over cmip5 models in simulating indian summer monsoon rainfall. *Atmospheric Research*, *232*, 104680.

Hanf, F. S., & Annamalai, H. (2020). Systematic errors in south asian monsoon precipitation: Process-based diagnostics and sensitivity to entrainment in ncar models. *Journal of Climate*, *33*(7), 2817–2840.

Hari, V., Villarini, G., Karmakar, S., Wilcox, L. J., & Collins, M. (2020). Northward propagation of the intertropical convergence zone and strengthening of indian summer monsoon rainfall. *Geophysical research letters*, *47*(23), e2020GL089823.

He, L., Zhou, T., & Chen, X. (2022). South asian summer rainfall from cmip3 to cmip6 models: biases and improvements. *Climate Dynamics*, 1–13.

Hersbach, H., Bell, B., Berrisford, P., Hirahara, S., Horányi, A., Muñoz-Sabater, J., ... others (2020). The era5 global reanalysis. *Quarterly Journal of the Royal Meteorological Society*, *146*(730), 1999–2049.

Hill, S. A. (2019). Theories for past and future monsoon rainfall changes. *Current Climate Change Reports*, *5*, 160–171.

Huang, B., Banzon, V. F., Freeman, E., Lawrimore, J., Liu, W., Peterson, T. C., ... Zhang, H.-M. (2015). Extended reconstructed sea surface temperature version 4 (ersst. v4). part i: Upgrades and intercomparisons. *Journal of climate*, *28*(3), 911–930.

Jain, S., Mishra, S. K., Anand, A., Salunke, P., & Fasullo, J. T. (2021). Historical and projected low-frequency variability in the somali jet and indian summer monsoon. *Climate Dynamics*, *56*, 749–765.

Jian, B., Li, J., Wang, G., Zhao, Y., Li, Y., Wang, J., ... Huang, J. (2021). Evaluation of the cmip6 marine subtropical stratocumulus cloud albedo and its controlling factors. *Atmospheric Chemistry and Physics*, *21*(12), 9809–9828.

Kang, S. M., Frierson, D. M., & Held, I. M. (2009). The tropical response to extratropical thermal forcing in an idealized gcm: The importance of radiative feedbacks and convective parameterization. *Journal of the atmospheric sciences*, *66*(9), 2812–2827.

Katzenberger, A., Schewe, J., Pongratz, J., & Levermann, A. (2021). Robust increase of indian monsoon rainfall and its variability under future warming in cmip6 models. *Earth System Dynamics*, *12*(2), 367–386.

Kay, J. E., Holland, M. M., Bitz, C. M., Blanchard-Wrigglesworth, E., Gettelman, A., Conley, A., & Bailey, D. (2012). The influence of local feedbacks and northward heat transport on the equilibrium arctic climate response to increased greenhouse gas forcing. *Journal of Climate*, *25*(16), 5433–5450.

Kim, H., Kang, S. M., Kay, J. E., & Xie, S.-P. (2022). Subtropical clouds key to southern ocean teleconnections to the tropical pacific. *Proceedings of the National Academy of Sciences*, *119*(34), e2200514119.

Konda, G., & Vissa, N. K. (2022). Evaluation of cmip6 models for simulations of surplus/deficit summer monsoon conditions over india. *Climate Dynamics*, 1–20.

Krishna, R. P. M., Rao, S. A., Srivastava, A., Kottu, H. P., Pradhan, M., Pillai, P., . . . Sabeerali, C. (2019). Impact of convective parameterization on the seasonal prediction skill of indian summer monsoon. *Climate Dynamics*, *53*, 6227–6243.

Kumar, T. L., Vinodhkumar, B., Rao, K. K., Chowdary, J., Osuri, K. K., & Desamsetti, S. (2023). Insights from the bias-corrected simulations of cmip6 in india's future climate. *Global and Planetary Change*, *226*, 104137.

Levine, R. C., Turner, A. G., Marathayil, D., & Martin, G. M. (2013). The role of northern arabian sea surface temperature biases in cmip5 model simulations and future projections of indian summer monsoon rainfall. *Climate dynamics*, *41*, 155–172.

Li, J.-L., Waliser, D., Stephens, G., Lee, S., L'Ecuyer, T., Kato, S., . . . Ma, H.-Y. (2013). Characterizing and understanding radiation budget biases in cmip3/cmip5 gcms, contemporary gcm, and reanalysis. *Journal of Geophysical Research: Atmospheres*, *118*(15), 8166–8184.

Li, J.-L., Xu, K.-M., Jiang, J., Lee, W.-L., Wang, L.-C., Yu, J.-Y., . . . Wang, Y.-H. (2020). An overview of cmip5 and cmip6 simulated cloud ice, radiation fields, surface wind stress, sea surface temperatures, and precipitation over tropical and subtropical oceans. *Journal of Geophysical Research: Atmospheres*, *125*(15), e2020JD032848.

Loeb, N. G., Doelling, D. R., Wang, H., Su, W., Nguyen, C., Corbett, J. G., . . . Kato, S. (2018). Clouds and the earth's radiant energy system (ceres) energy balanced and filled (ebaf) top-of-atmosphere (toa) edition-4.0 data product. *Journal of Climate*, *31*(2), 895–918.

Mitra, A. (2021). A comparative study on the skill of cmip6 models to preserve daily spatial patterns of monsoon rainfall over india. *Frontiers in Climate*, *3*, 654763.

Pillai, P. A., Rao, S. A., Ramu, D. A., Pradhan, M., & George, G. (2018). Seasonal prediction skill of indian summer monsoon rainfall in nmme models and monsoon mission cfsv2. *International Journal of Climatology*, *38*, e847–e861.

Planton, Y. Y., Guilyardi, E., Wittenberg, A. T., Lee, J., Gleckler, P. J., Bayr, T., . . . others (2021). Evaluating climate models with the clivar 2020 enso metrics package. *Bulletin of the American Meteorological Society*, *102*(2), E193–E217.

Rajendran, K., Surendran, S., Varghese, S. J., & Sathyanath, A. (2022). Simulation of indian summer monsoon rainfall, interannual variability and teleconnections: evaluation of cmip6 models. *Climate Dynamics*, *58*(9-10), 2693–2723.

Schneider, T., Bischoff, T., & Haug, G. H. (2014). Migrations and dynamics of the intertropical convergence zone. *Nature*, *513*(7516), 45–53.

Tanaka, H. L., Ishizaki, N., & Kitoh, A. (2004). Trend and interannual variability of walker, monsoon and hadley circulations defined by velocity potential in the upper troposphere. *Tellus A: Dynamic Meteorology and Oceanography*, *56*(3), 250–269.

Vecchi, G. A., & Soden, B. J. (2007). Global warming and the weakening of the tropical circulation. *Journal of Climate*, *20*(17), 4316–4340.

Voigt, A., Biasutti, M., Scheff, J., Bader, J., Bordoni, S., Codron, F., … others (2016). The tropical rain belts with an annual cycle and a continent model intercomparison project: Tracmip. *Journal of Advances in Modeling Earth Systems*, *8*(4), 1868–1891.

Walker, G. (1923). Correlation in seasonal variations of weather, viii: A preliminary study of weather. *Mem. Indian Meteor. Dep*, *24*, 75–131.

Xiang, B., Zhao, M., Ming, Y., Yu, W., & Kang, S. M. (2018). Contrasting impacts of radiative forcing in the southern ocean versus southern tropics on itcz position and energy transport in one gfdl climate model. *Journal of Climate*, *31*(14), 5609–5628.

Xiao, H., Mechoso, C. R., Sun, R., Han, J., Pan, H.-L., Park, S., … Teixeira, J. (2014). Diagnosis of the marine low cloud simulation in the ncar community earth system model (cesm) and the ncep global forecast system (gfs)-modular ocean model v4 (mom4) coupled model. *Climate dynamics*, *43*, 737–752.

Zhao, L., Wang, Y., Zhao, C., Dong, X., & Yung, Y. L. (2022). Compensating errors in cloud radiative and physical properties over the southern ocean in the cmip6 climate models. *Advances in Atmospheric Sciences*, *39*(12), 2156–2171.

Supporting Information for South Asian Summer Monsoon Precipitation is Sensitive to Southern Hemisphere Subtropical Radiation Changes

Dipti Hingmire[1], Haruki Hirasawa[1], Hansi Singh[1,5], Philip J. Rasch[2],

Sookyung Kim[3,6], Subhashis Hazarika[3,6], Peetak Mitra[3,4], Kalai Ramea[3,5]

[1]School of Earth and Ocean Sciences, University of Victoria, Victoria, BC, Canada

[2]Department of Atmospheric Sciences, University of Washington, Seattle, WA, USA

[3]Palo Alto Research Corporation, Palo Alto, CA, USA

[4]Excarta, Palo Alto, CA, USA

[5]Planette Inc., San Francisco, CA, USA

[6]SRI International, Palo Alto, CA, USA

Contents of this file

Description of observations and reanalysis data

Monthly observation data used in this study includes precipitation from the Global Precipitation Climatology Project version 2.3 (GPCP; Adler et al. (2018)), Sea Surface Temperature (SST) data from Extended Reconstructed Sea Surface Temperature (ERSST), version 4 (Huang et al., 2015) and Top Of Atmosphere (TOA) radiation fluxes from Clouds and the Earth's Radiant Energy System Energy Balanced and Filled (CERES-EBAF) version 4.2 (Loeb et al., 2018). Gridded reanalyzed upper-air circulation products used in the study were obtained from the European Centre for Medium-Range Weather Forecasts (ECMWF) ERA5 (Hersbach et al., 2020). To calculate biases in the CESM2 we used 11 historical simulations from CMIP6 archive. The biases are calculated as the climatological mean difference between model and observations for the period 1979-2014, except for TOA radiation fluxes where we use climatology of 2004-2014, as the CERES instrument was launched in 1999.

CMIP6 Data

We used historical monthly data from 11 ensemble members of CESM2 (Danabasoglu et al., 2020) participating in CMIP6 to analyse the existing CESM2 biases. To calculate multimodel regression of SASM precipitation biases onto net TOA biases we used 32 CMIP6 (Eyring et al., 2016) ESMs as listed in table S1.

Figure Descriptions

Figures S1 to S8 provide additional support and insights on the findings detailed in the main text. The F_{TOA} response of fixing CDNC to 150 cm^{-3} for Atlantic and 75 cm^{-3} in other experiments is shown in Figure S1. Fixing CDNC produces a reduction of 4-12 Wm^{-2} in F_{TOA} radiation over the SH subtropical region (panels e-h Figure S1). Figure S2 shows the existing biases in the CESM2 with GPCP for different monsoon regions of the world. The CESM2 have biases in simulating climatological mean precipitation for other monsoon regions as well. Figures S3 to S7 show precipitation response of the radiation reduction experiments over other monsoon regions. For West African monsoon during May-June and July to September, the Atlantic experiment improves the Sahel precipitation bias by small amount while as other experiments have negligible effects (Figures S3 and S4). All the experiments show worsening of biases of southern hemisphere monsoons such as Australian monsoon and East/South African monsoon in December-February, (Figures S5 and S6) with exception of South American monsoon for which the Atlantic experiment shows improvement in precipitation biases over Brazil (Figure S7). Figure S8 depicts the relationship between Root Mean Square Errors (RMSE, calculated with GPCP for precipitation and CERES-EBAF for radiation) in net TOA and SASM precipitation for CMIP6 multimodel ensemble. The models having higher RMSE in SASM precipitation show errors in SH subtropical net TOA as well.

References

Adler, R. F., Sapiano, M. R., Huffman, G. J., Wang, J.-J., Gu, G., Bolvin, D., ... others (2018). The global precipitation climatology project (gpcp) monthly analysis (new version 2.3) and a review of 2017 global precipitation. *Atmosphere*, *9*(4), 138.

Danabasoglu, G., Lamarque, J.-F., Bacmeister, J., Bailey, D., DuVivier, A., Edwards, J., ... others (2020). The community earth system model version 2 (cesm2). *Journal of Advances in Modeling Earth Systems*, *12*(2), e2019MS001916.

Eyring, V., Bony, S., Meehl, G. A., Senior, C. A., Stevens, B., Stouffer, R. J., & Taylor, K. E. (2016). Overview of the coupled model intercomparison project phase 6 (cmip6) experimental design and organization. *Geoscientific Model Development*, *9*(5), 1937–1958.

Hersbach, H., Bell, B., Berrisford, P., Hirahara, S., Horányi, A., Muñoz-Sabater, J., ... others (2020). The era5 global reanalysis. *Quarterly Journal of the Royal*

Meteorological Society, *146*(730), 1999–2049.

Huang, B., Banzon, V. F., Freeman, E., Lawrimore, J., Liu, W., Peterson, T. C., ... Zhang, H.-M. (2015). Extended reconstructed sea surface temperature version 4 (ersst. v4). part i: Upgrades and intercomparisons. *Journal of climate*, *28*(3), 911–930.

Loeb, N. G., Doelling, D. R., Wang, H., Su, W., Nguyen, C., Corbett, J. G., ... Kato, S. (2018). Clouds and the earth's radiant energy system (ceres) energy balanced and filled (ebaf) top-of-atmosphere (toa) edition-4.0 data product. *Journal of Climate*, *31*(2), 895–918.

Table S1. CMIP6 models used in this study

CMIP6 model	Ensemble member	CMIP6 model	Ensemble member
ACCESS-CM2	r1i1p1f1	E3SM-1-1	r1i1p1f1
ACCESS-ESM1-5	r1i1p1f1	E3SM-1-1-ECA	r1i1p1f1
AWI-CM-1-1-MR	r1i1p1f1	EC-Earth3-Veg-LR	r1i1p1f1
AWI-ESM-1-1-LR	r1i1p1f1	FGOALS-g3	r1i1p1f1
BCC-CSM2-MR	r1i1p1f1	GFDL-CM4	r1i1p1f1
BCC-ESM1	r1i1p1f1	GFDL-ESM4	r1i1p1f1
CESM2	r1i1p1f1	GISS-E2-1-G-CC	r1i1p1f1
CESM2-FV2	r1i1p1f1	INM-CM4-8	r1i1p1f1
CESM2-WACCM	r1i1p1f1	IPSL-CM6A-LR	r1i1p1f1
CESM2-WACCM-FV2	r1i1p1f1	MIROC-ES2L	r1i1p1f2
CMCC-CM2-SR5	r1i1p1f1	MIROC6	r1i1p1f1
CNRM-CM6-1	r1i1p1f2	MPI-ESM1-2-LR	r1i1p1f1
CNRM-CM6-1-HR	r1i1p1f2	MRI-ESM2-0	r1i1p1f1
CNRM-ESM2-1	r1i1p1f2	NESM3	r1i1p1f1
CanESM5-CanOE	r1i1p2f1	NorESM2-MM	r1i1p1f1
TaiESM1	r1i1p1f1	SAM0-UNICON	r1i1p1f1

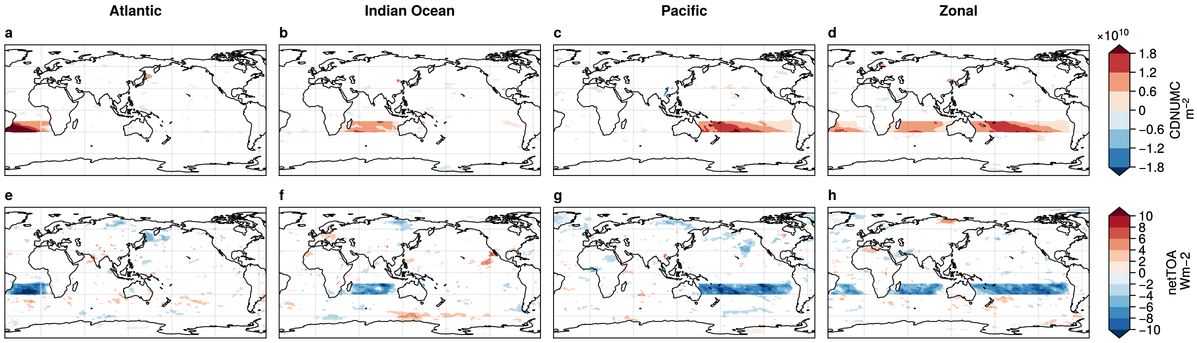

Figure S1. Fixed-SST response: Applied CDNC perturbations (cm^{-3}; a-d) and annual mean changes in F_{TOA} radiation (W m^{-2}; e-h) in fixed-SST simulations over different regions - (a,e) Atlantic, (b,f) Indian Ocean, (c,g) Pacific and (d,h) Zonal. Only significant ($p < 0.05$) changes are shown in colour.

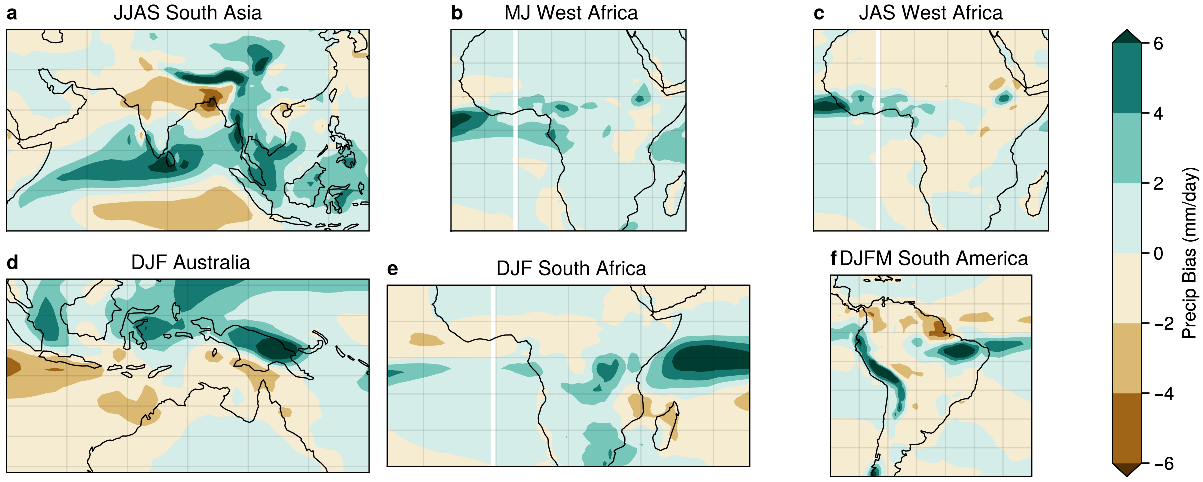

Figure S2. **Existing biases in CESM2:** Ensemble mean bias of CESM2 Precipitation with GPCP (mm/day) for a. June-September (JJAS) over South Asia, b. May-June (MJ) over West Africa, c. July-September (JAS) over West Africa, d. December-February (DJF) over Australia, e. DJF over South Africa and f. December-March (DJFM) over South America.

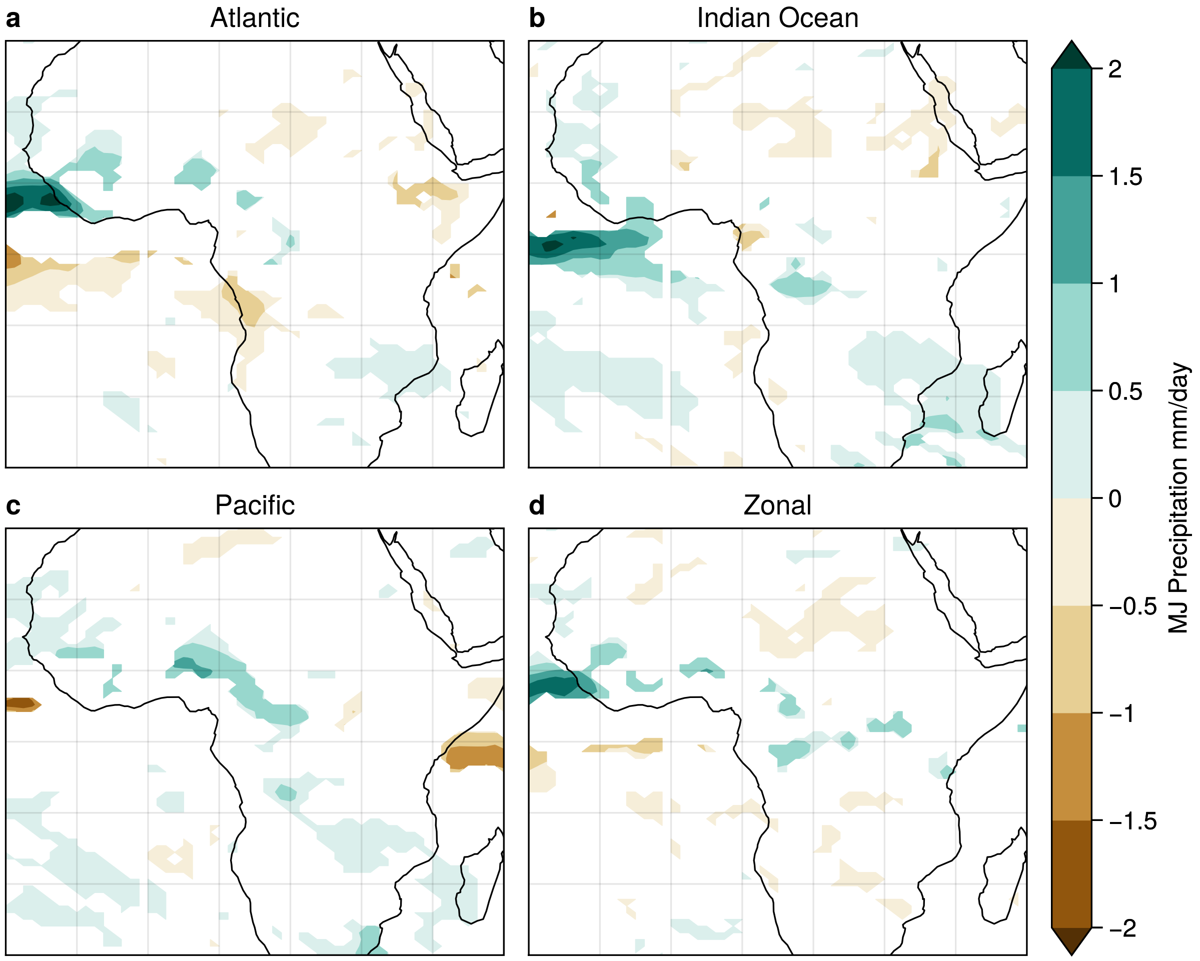

Figure S3. West African precipitation response: MJ precipitation response (mm/day) (at simulation period 121-150 years) in fully coupled simulation for experiments a. Atlantic, b. Indian Ocean, c. Pacific and d. Zonal. Non-significant responses (at level of significance 0.05) are masked in white.

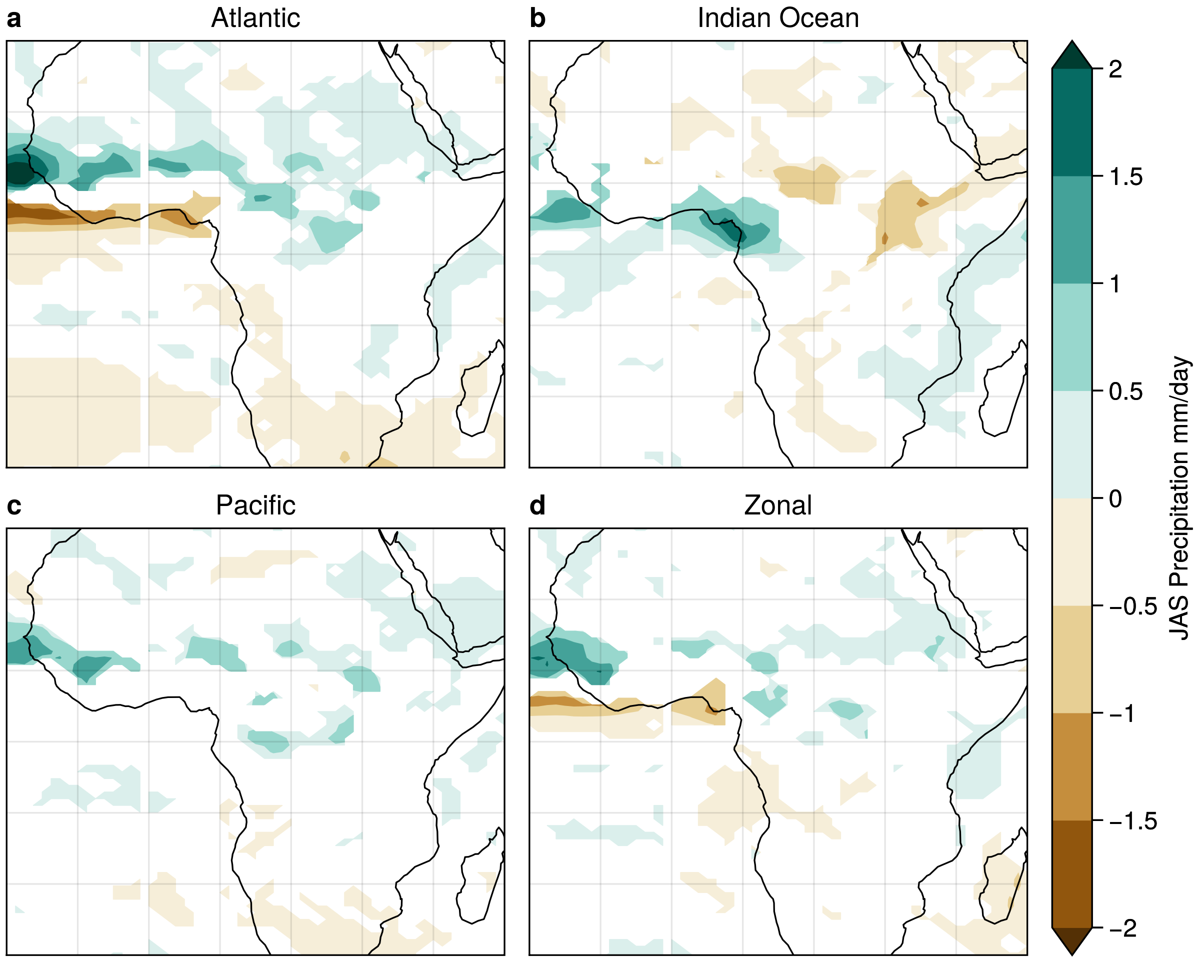

Figure S4. West African precipitation response: JAS precipitation response (mm/day) (at simulation period 121-150 years) in fully coupled simulation for experiments a. Atlantic, b. Indian Ocean, c. Pacific and d. Zonal. Non-significant responses (at level of significance 0.05) are masked in white.

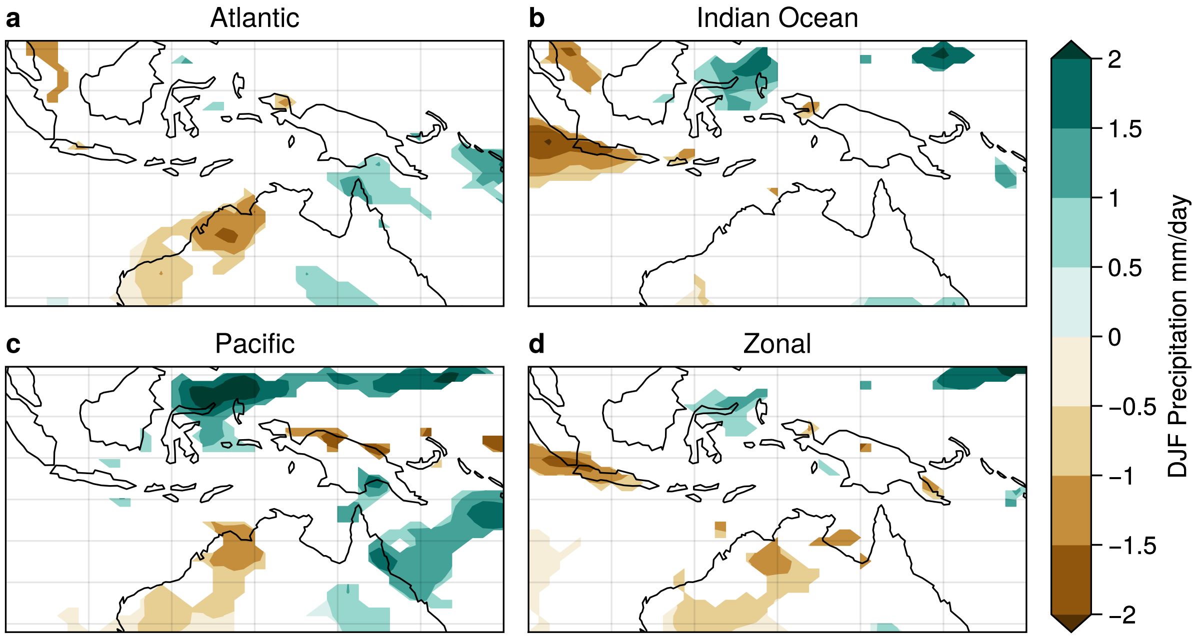

Figure S5. Australian monsoon precipitation response: DJF precipitation response (mm/day) (at simulation period 121-150 years) in fully coupled simulation for experiments a. Atlantic, b. Indian Ocean, c. Pacific and d. Zonal. Non-significant responses (at level of significance 0.05) are masked in white.

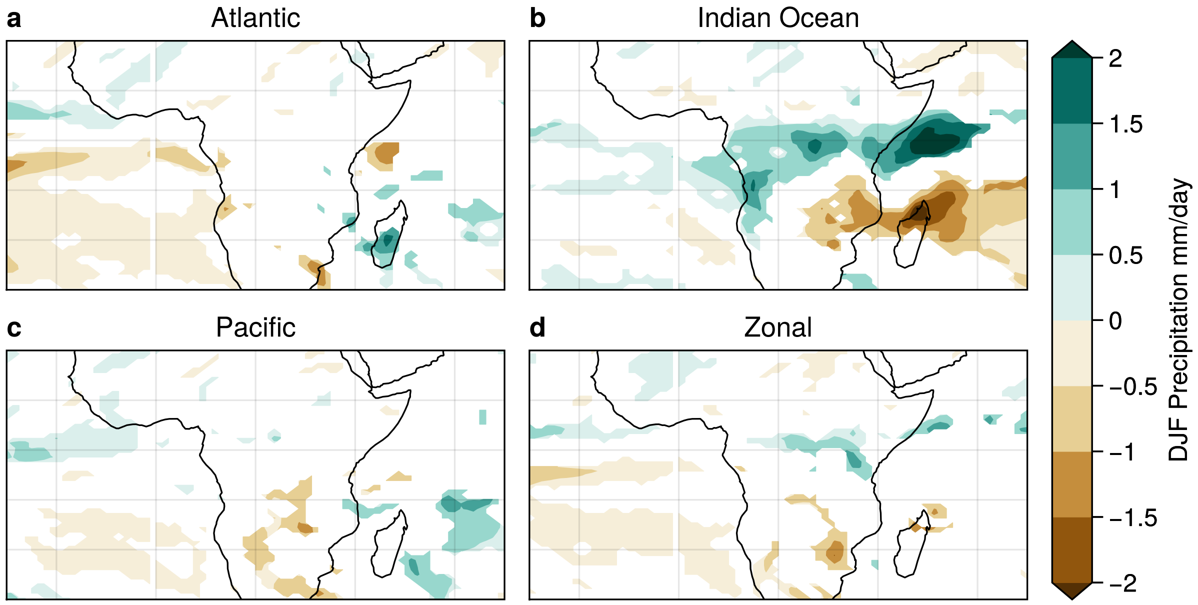

Figure S6. East African monsoon precipitation response: DJF precipitation response (mm/day) (at simulation period 121-150 years) in fully coupled simulation for experiments a. Atlantic, b. Indian Ocean, c. Pacific and d. Zonal. Non-significant responses (at level of significance 0.05) are masked in white.

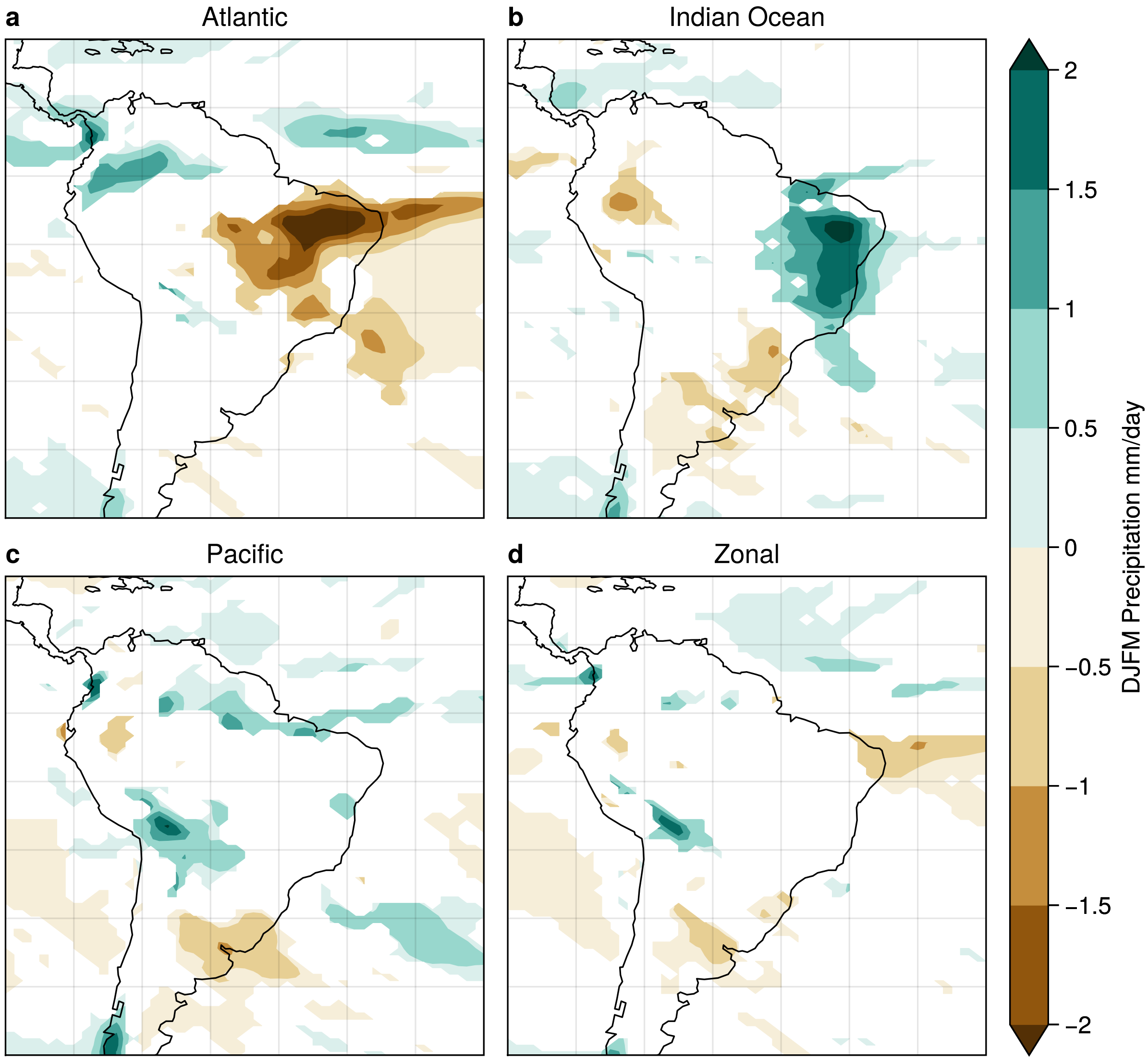

Figure S7. South American monsoon precipitation response: DJFM precipitation response (mm/day) (at simulation period 121-150 years) in fully coupled simulation for experiments a. Atlantic, b. Indian Ocean, c. Pacific and d. Zonal. Non-significant responses (at level of significance 0.05) are masked in white.

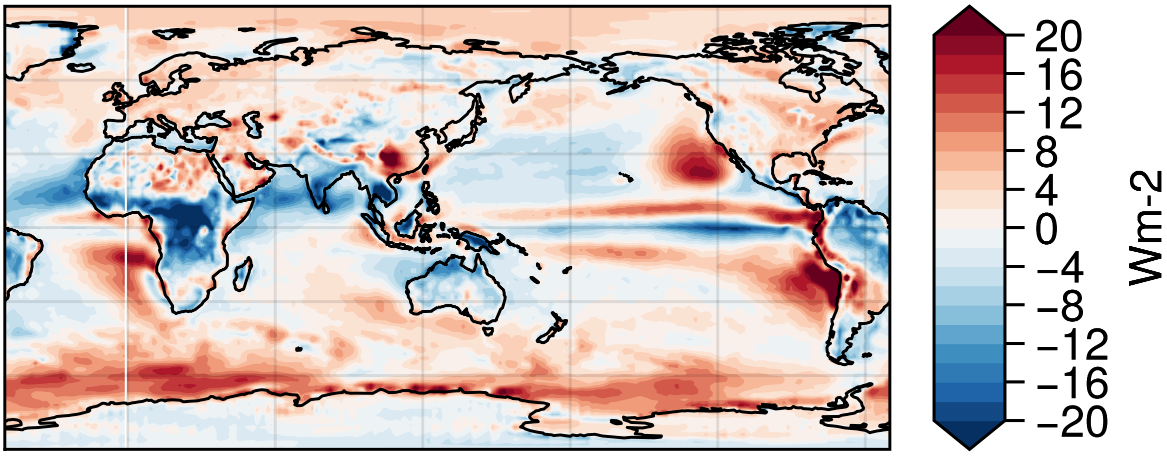

Figure S8. Regression of net TOA Root Mean Square Errors (RMSE) (W m^{-2}) and SASM precipitation RMSE (mm day^{-1}) in the CMIP6 multi-model ensemble evaluated when SASM precipitation RMSE is two standard deviations above the multi-model mean.